

## Author's Response to all comments:

### Response to Anonymous Referee #1

We would first like to thank the anonymous referee for his or her constructive comments. In this response we will try to answer all the comments and the indicated changes will be applied in the revised manuscript.

**General comment:** *“However, I have a suggestion that the global results should be presented and compared in a clearer manner. Currently, global erosion estimates were presented only in Table 7; no global map of erosion estimations were presented (only specific factors).”*

**Answer:** We did not present a global map of soil erosion rates, due to the fact that the other RUSLE factors (K, C and P) are not adjusted to the coarse resolution for global scale application as the S and R factors. We wanted to stress the improvements made by adjusting the S and R factors, rather than focusing on the final soil erosion rates. However, we agree that providing global maps of erosion rates can help making the statistics in table 7 point out the improvements made in this study in a clearer way. So, additional to table 7, we will include in the revised version of this article 4 maps of global soil erosion rates. One map showing the erosion rates for the fully adjusted RUSLE model (Fig. 8A). The second map will show a difference plot between the fully adjusted and unadjusted RUSLE model (Fig. 8B). The third map will show a difference plot between the RUSLE model with only adjusted S factor and the unadjusted RUSLE model (Fig. 8C). And finally the last map will show a difference plot between the RUSLE model with only adjusted R factor and the unadjusted RUSLE model (Fig. 8D). These maps should highlight the different contributions of the adjusted S and R factors on erosion rates for the global scale. See changes in the revised manuscript.

**Specific comment 1:** *Page 3003 Line 15–16 It seems that the two variables, annual precipitation and precipitation intensity, are not independent each other. Did you check independence among the variables used in the regression analysis?*

**Answer:** We checked the independence of these variables and they are in some extent correlated, because the precipitation intensity is inferred from the long term total precipitation on wet days. We found an r squared of 0.5 when plotting the two variables against each other. However, these two variables contain different information. For example the precipitation intensity is shown to

be crucial in a lot of climate zones (see for example the case of the Ebro basin in Spain). Also, the annual total precipitation provides additional information which makes the regression more accurate. Without the annual precipitation, the performance of the multiple regression approach is lower. So we decided that both variables play an important role in the multiple regression approach.

**Specific comment 2:** *Page 3007 Line 14 I have some concern about the statement that “... and support practice (P) factors do not contribute significantly to the variation in soil erosion at the continental scale.” As you know, much efforts of soil management practice have been made to prevent erosion. In other words, I’m worrying about over-fitting in this study by putting too much focus on S and R factors.*

**Answer:** We understand that this sentence may be misleading, management contributes a lot in preventing soil erosion in agricultural areas; however, the uncertainty in estimating the P factor due to the lack of data is large. Including this factor in the erosion estimations would mean including an additional large source of uncertainty. And as we want to keep the model simple and focus on presenting the improvements made to the S and R factors, we left this factor out of the calculations. We reformulate the sentence in the revised manuscript and add additional information explaining in a more detailed way like above why we ignored the L and P factors in our calculations.

**Specific comment 3:** *Page 3007 Line 23–15 As mentioned above, presentation of the global results is not adequate for me. I suggest adding further comparisons among the simulations, such as global map and latitudinal distribution.*

**Answer:** See answer to general comment

**Specific comment 4:** *Page 3018 Table1 The column “Temporal resolution” does not provide temporal resolution (e.g., daily, monthly, annual) but show only temporal period. Please correct the label or data in the column.*

**Answer:** Changed accordingly

**Specific comment 5:** *Page 3022 Table 5 Can you show R results by the unadjusted model for comparison?*

**Answer:** Yes, we provide in the revised manuscript in Table 6 the R values as originally calculated by Renard and Freimund

## **Response to Anonymous Referee #2**

We would first like to thank the anonymous referee for his or her helpful comments. In this response we will try to answer these comments and the indicated changes will be applied in the revised manuscript.

**Comment 1:** *Abstract: line 5, sentence word order a little scrambled, '(RUSLE) model is due to...' add comma after model, and move 'is' to after 'basis,'*

**Answer:** Abstract, line 5, sentence “(RUSLE) model is due to its simple structure and empirical basis a frequently used tool” is changed to “(RUSLE) model, due to its simple structure and empirical basis, is a frequently used tool” in the revised manuscript.

**Comment 2:** *Abstract: line 17, word order, reverse 'in' and 'good'*

**Answer:** Abstract, line 17, sentence “resulted in values that are in good comparison with high resolution” is changed to “resulted in values that compared well to high resolution” in the revised manuscript.

**Comment 3:** *Introduction: line 12, biogeochemical components have become increasingly important - add references.*

**Answer:** We add the following references in the revised manuscript after line 12: Thornton et al. (2007) and Goll et al. (2012)

**Comment 4:** *Pg 2998, line 14 - why is a 3x3 pixel window chosen? Is it purely because this is the smallest moving window? What is the influence of this choice? Can changing window size in different topographical regions help?*

**Answer:** As discussed in Zhang et al. (1999), a 3x3 pixel window is chosen mainly because of two reasons. First, it is the smallest moving window, secondly, it is assumed that the fractal coefficient  $\alpha$  and fractal dimension  $D$  are stable in this 3x3 pixel window. The last assumption is essential here, because the fractal method of scaling slope is mainly based on this assumption. If one would increase the moving window size, the fractal parameters could be less stable, independent of the topographical region. We already see that although we assume that in a 3x3

pixel window the fractal coefficients are stable, they actually change a little bit. This effect would increase with increasing moving window. Also, this effect is more pronounced in topographically complex regions.

**Comment 5:** *Figure 2: I would find it useful if the original RUSLE estimation was shown as well as a difference. Figure 2: caption 'redisch'*

**Answer:** We add in the revised manuscript the unscaled global slope in Figure 2A and keep the difference plot in Figure 2B. “Redisch” is corrected by “Reddish” in the revised manuscript.

**Comment 6:** *Figure 3 and 6: Why is Switzerland presented differently to the other two regions? I would prefer a uniform representation, unless there is a rational for this, in which case it should be presented.*

**Answer:** We guess you mean not Switzerland but the Ebro basin in Spain that is presented differently. This is due to the fact that we cannot have access to the original erosivity data of the Ebro basin (presented in the study of Angulo-Martinez et al., 2009) and thus cannot make a difference plot such as the figures of the USA and Switzerland. We state this explicitly in the revised manuscript in the description of figure 6.

**Comment 7:** *Figure 4: more explanation of figure in the caption would be useful.*

**Answer:** We add an additional table (Table 3) with definitions for all climate zones as presented in Peel et al. (2007) in the revised manuscript. The rest of the tables in the manuscript are renumbered.

**Comment 8:** *Pg 3004, line 5, how is this evaluated? Using the r squared? In how many cases are the Renard Freimund R factors kept?*

**Answer:** Yes, we mainly used the r squared combined with the residual standard error to evaluate if the improvement of the R factor was significant. If the r squared value of the regression method was significantly different from the method of Renard and Freimund, then the regression method was preferred. In case there was not much difference in the r squared values between the methods, we looked at the differences in the residual standard error. In case of the E climates, the r squared was low for both methods, so we also compared the mean R values of these climates to the observed ones to see if there was improvement. The Renard and Freimund R factors are first of all kept for climate zones where we had no or too less high resolution data.

From the climate zones where we had high resolution data, the Renard and Freimund R factors were kept for the BWh and Csa climates. These are just 2 climate zones out of 17. Although the Renard and Freimund method performed badly for the Csa climate, no improvement was found with the multiple regression approach. For the BWh the Renard and Freimund method performed slightly better than for the Csa climate, and the multiple regression approach did not change this result significantly.

We will highlight this in the revised manuscript.

**Comment 9:** *Climate zones - I struggled to find a definition of the climate zones to begin with, but I see there's a description of some of the zones in Table 5. Signposting the reader to the definitions earlier in the text would be helpful, and providing definitions for all the climate zone codes would also be useful.*

**Answer:** See answer to comment 7. We also refer to the new table with definitions for the climate zones in the revised manuscript.

**Comment 10:** *Pg 3004, line 22, should this be Table 5 rather than 3?*

**Answer:** We can see the point you are making here. Both Table 3 and 5 in the manuscript show that the f climate zones can be explained by the total yearly precipitation and the SDII. Table 3 shows which the significant parameters are for the f climate zones, while table 5 shows that for these climate zones the regression performs well when compared to high resolution erosivity for the USA. We refer to both tables in the revised manuscript.

**Comment 11:** *Figures 5 needs to be improved. The layout and sizing of the plots needs to be consistent. I would find it easier to evaluate the results if the plots were given equal axes such that the one-to-one line always lies on the 45 degree diagonal, and the axes were the same between 1 and 2. Units should be mentioned.*

**Answer:** The sizing of figures 5 is improved to be more consistent in the revised manuscript. It was for us difficult to give all the plots equal axes, due to the fact that the correlation becomes much less visible. Also one is not able to see anymore how the data is spread, and in which way the different methods overestimate or underestimate the observed R values. In these plots it is most important to see how the observed R values correlate with the modelled ones from the different methods for a specific climate zone. In some cases the modelled R values are much

larger than the observed ones, which make it difficult to use equal axes and equal spacing between the axis ticks. Finally, one needs to keep in mind that the red line always lays on the 45 degree diagonal. In the description of figure 5 in the revised manuscript we add the units and explicitly mention that the red line always lies on the 45 degree diagonal.

**Comment 12:** *Figure 6 and text that refers to it, care should be taken to highlight that Switzerland is no longer a truly independent test given that this data has been used in the regressions. This doesn't invalidate the work, the improvements for Spain are impressive, but it should be discussed.*

**Answer:** We mention in the revised manuscript about the fact that Switzerland is not an independent case study anymore after the regression. We also mention that in the Ebro basin in Spain the E climate zones, for which the R factor was adjusted in Switzerland, also occur. And there the improvement is also clearly visible.

**Comment 13:** *Section 4.2: I think it's important to provide mapped results for the erosion models as this is the end point for the work. Means do not tell the whole story and mapped output would help illustrate the discussion.*

**Answer:** We did not present a global map of soil erosion rates, due to the fact that the other RUSLE factors (K, C and P) are not adjusted to the coarse resolution for global scale application as the S and R factors. We wanted to stress the improvements made by adjusting the S and R factors, rather than focusing on the final soil erosion rates. However, we agree that providing global maps of erosion rates can help making the statistics in table 7 point out the improvements made in this study in a clearer way. So, additional to table 7 (of the original manuscript), we include in the revised version of this article 4 maps of global soil erosion rates. One map showing the erosion rates for the fully adjusted RUSLE model (Fig. 8A). The second map will show a difference plot between the fully adjusted and unadjusted RUSLE model (Fig. 8B). The third map will show a difference plot between the RUSLE model with only adjusted S factor and the unadjusted RUSLE model (Fig. 8C). And finally the last map will show a difference plot between the RUSLE model with only adjusted R factor and the unadjusted RUSLE model (Fig. 8D). These maps should highlight the different contributions of the adjusted S and R factors on erosion rates for the global scale. See changes in the revised manuscript.

**Comment 14:** *Pg 3008, line 19, What's happened in the north west of the US with the adjusted model? Perhaps the authors can comment.*

**Answer:** See explanation in the revised manuscript

**Comment 15:** *Perhaps the authors can comment on using the RUSLE which gives a erosion rate for an average annual climate and then comparing that*

**Answer:** We are sorry, but unfortunately we do not understand, what the referee means here.

**Comment 16:** *Pg 3009 Can you say something more definitive here? You can see where the model is overestimating, and you know the K and C factors for these areas - are there trends here, i.e. is it systematically overestimating in regions dominated by arable land covers?*

**Answer:** We shortly took a look at how the adjusted RUSLE model performs for different land cover types in the USA and Europe and didn't see a clear signal where the RUSLE performs worse and where better. The global maps on erosion rates from the new figures can provide some insight here as they can make the analysis spatially explicit. In general, we see that the adjusted RUSLE model still overestimates erosion rates for most land cover types. However, when taking a more accurate look the largest biases are found for shrubs, and the least for grassland. A lot of factors play a role here, for example it is important to consider where the land use is allocated. On steep hillslopes the effect on erosion would be different than in flat areas. So a more explicit analysis is needed here to find out how we can improve the contribution of land cover and land use to erosion rates in the RUSLE model. See the revised manuscript for the changes made.

**Comment 17:** Pg 3011, line 21 spelling: performs

**Answer:** Changed accordingly

1  
2  
3  
4  
5

6 **Revised Manuscript**

7

8 **Improving the global applicability of the RUSLE model –**

9 **Adjustment of the topographical and rainfall erosivity factors**

10

11 V. Naipal<sup>1</sup>, C. Reick<sup>1</sup>, J. Pongratz<sup>1</sup>, K. Van Oost<sup>2</sup>

12 [1] {Max Planck Institute for Meteorology, Hamburg 20146, Germany}

13 [2] {Université catholique de Louvain, TECLIM – Georges Lemaître Centre for Earth and  
14 Climate Research, Louvain-la-Neuve, Belgium}

15 Received: 12 February 2015 – Accepted: 6 March 2015 – Published: 19 March 2015

16 Correspondence to: V. Naipal (victoria.naipal@mpimet.mpg.de)

17 Published by Copernicus Publications on behalf of the European Geosciences Union

18

19 **Abstract**

20 Large uncertainties exist in estimated rates and the extent of soil erosion by surface runoff on a  
21 global scale, and this limits our understanding of the global impact that soil erosion might have  
22 on agriculture and climate. The Revised Universal Soil Loss Equation (RUSLE) model ~~is~~ due to  
23 its simple structure and empirical basis is a frequently used tool in estimating average annual  
24 soil erosion rates at regional to global scales. However, large spatial scale applications often rely  
25 on coarse data input, which is not compatible with the local scale at which the model is  
26 parameterized. This study aimed at providing the first steps in improving the global applicability  
27 of the RUSLE model in order to derive more accurate global soil erosion rates.

28 We adjusted the topographical and rainfall erosivity factors of the RUSLE model and compared  
29 the resulting soil erosion rates to extensive empirical databases on soil erosion from the USA and  
30 Europe. Adjusting the topographical factor required scaling of slope according to the fractal



31 method, which resulted in improved topographical detail in a coarse resolution global digital  
32 elevation model.

33 Applying the linear multiple regression method to adjust rainfall erosivity for various climate  
34 zones resulted in values that ~~are in good comparison with~~ compared well to high resolution  
35 erosivity data for different regions. However, this method needs to be extended to tropical  
36 climates, for which erosivity is biased due to the lack of high resolution erosivity data.

37 After applying the adjusted and the unadjusted versions of the RUSLE model on a global scale  
38 we find that the adjusted RUSLE model not only shows a global higher mean soil erosion rate  
39 but also more variability in the soil erosion rates. Comparison to empirical datasets of the USA  
40 and Europe shows that the adjusted RUSLE model is able to decrease the very high erosion rates  
41 in hilly regions that are observed in the unadjusted RUSLE model results. Although there are still  
42 some regional differences with the empirical databases, the results indicate that the methods used  
43 here seem to be a promising tool in improving the applicability of the RUSLE model on a coarse  
44 resolution on global scale.

45

## 46 **1 Introduction**

47 For the last centuries to millennia soil erosion by surface runoff is being accelerated globally due  
48 to human activities, such as deforestation and agricultural practices (Bork and Lang, 2003).  
49 Accelerated soil erosion is a process that triggers land degradation in the form of nutrient loss, a  
50 decrease in the effective root depth, water imbalance in the root zone and finally also  
51 productivity reduction (Yang et al., 2003). It is widely recognized that soil erosion is a major  
52 threat to sustainable agriculture and food production across the globe for many decades. These  
53 effects of soil erosion are currently exacerbated by the global population growth and climatic  
54 changes. Organizations such as the United Nations Convention to Combat Desertification  
55 (UNCCD) try to address this problem by stating a new goal for Rio +20 of zero land degradation  
56 (UNCCD, 2012).

57 Another aspect underpinning the relevance of soil erosion on the global scale is the effect of soil  
58 erosion on the global nutrient cycles. Recently, the biogeochemical components of Earth System  
59 Models (ESMs) became increasingly important in predicting the global future climate (Thornton

**Comment [VN1]:**

**Comment [3]: Reviewer #2:** add references

**Reply:** We add the following references in the revised manuscript after line 12: Thornton et al. (2007) and Goll et al. (2012)

60 | [et al., 2007](#); [Goll et al., 2012](#)). Not only the global carbon cycle but also other nutrient cycles  
61 such as the nitrogen (N) and phosphorous (P) cycles cannot be neglected in ESMs anymore (Goll  
62 et al.,2012; Gruber and Galloway, 2008; Reich et al., 2006). Soil erosion may have a significant  
63 impact on these nutrient cycles through lateral fluxes of sediment, but the impact on the global  
64 scale is still largely unknown. For example, Quinton et al. (2010) showed that erosion can  
65 significantly alter the nutrient and carbon cycling and result in lateral fluxes of nutrients that are  
66 similar in magnitude as fluxes induced by fertilizer application and crop removal. Regnier et al.  
67 (2013) looked at the effect of human induced lateral fluxes of carbon from land to ocean and  
68 concluded that human perturbations, which include soil erosion, may have enhanced the carbon  
69 export from soils to inland waters.

70 In general, the effect of soil erosion on the global carbon cycle has received considerable  
71 attention after the pioneering work of Stallard (1998), who proposed that global soil erosion can  
72 result in sequestration of carbon by soils. After his work, the effect of soil erosion on the carbon  
73 cycle has been studied extensively, but there remains a large uncertainty in the effect of soil  
74 erosion on the carbon cycle. For example, several recent global assessments of the influence of  
75 soil erosion on the carbon cycle indicate a large uncertainty with a range from a source of 0.37 to  
76 1 Pg C year<sup>-1</sup> to a net uptake or sink of 0.56 to 1 Pg C year<sup>-1</sup> (van Oost et al., 2007). Thus, in  
77 order to better constrain the global carbon budget and to identify optimal management strategies  
78 for land use, it is essential to have accurate estimates of soil erosion and its variability on a  
79 global scale.

80 Currently, however, there exists a large uncertainty in the global soil erosion rates as can be seen  
81 from recent studies that show rates between 20 and 200 Pg y<sup>-1</sup> (Doetterl et al., 2012). This  
82 indicates that modelling soil erosion on a global scale is still a difficult task due to the very high  
83 spatial and temporal variability of soil erosion. Different approaches were previously applied to  
84 estimate soil erosion on a large or global scale. Most of these approaches are based on  
85 extrapolated data from agricultural plots, sediment yield or extrapolated river sediment estimates  
86 (Milliman and Syvitski, 1992, Stallard, 1998, Lal, 2003, Hooke, 2000, Pimentel et al.,1995,  
87 Wilkinson and McElroy, 2007). An alternative approach is based on the use of soil erosion  
88 models. One of the most applied models to estimate soil erosion on a large spatial scale is the  
89 semi-empirical/process-based Revised Universal Soil Loss Equation (RUSLE) model (Renard et  
90 al., 1997). This model stems from the original Universal Soil Loss Equation (USLE) model

91 developed by USDA (USA Department of Agriculture), which is based on a large set of  
92 experiments on soil loss due to water erosion from agricultural plots in the United States (USA).  
93 These experiments covered a large variety of agricultural practices, soil types and climatic  
94 conditions, making it a potentially suitable tool on a regional to global scale. The RUSLE model  
95 predicts the average annual soil erosion rates by rainfall and is formulated as a product of a  
96 rainfall erosivity factor ( $R$ ), a slope steepness factor ( $S$ ), a slope length factor ( $L$ ), a soil  
97 erodibility factor ( $K$ ), a crop cover factor ( $C$ ) and a support practice factor ( $P$ ). The RUSLE  
98 model was first applied on a global scale by Yang et al. (2003) and Ito (2007) for estimating the  
99 global soil erosion potential and various limitations related to applying the RUSLE model on the  
100 global scale. Firstly, the model is originally developed to be applicable on the agricultural plot  
101 scale, which is not compatible with the coarse spatial scale of global datasets on soil erosion  
102 influencing factors such as precipitation, elevation, land-use and soil characteristics. Secondly,  
103 the RUSLE and USLE models were parameterized for environmental conditions of the United  
104 States (USA), and are thus not directly applicable to other areas in the world. Thirdly, only sheet  
105 and rill erosion are considered, and finally the RUSLE model does not contain sediment  
106 deposition and sediment transport terms, which are closely linked to soil erosion.

107 The RUSLE model is to our knowledge one of the few erosion models that has the potential to be  
108 applied on a global scale due to its simple structure and empirical basis. Therefore it is of key  
109 importance to address the above mentioned limitations first.

110 To address the first two limitations, Van Oost et al. (2007) presented in their work a modified  
111 version of the USLE model for application on agricultural areas on a global scale. They based  
112 their model on large-scale experimental soil erosion data from the USA (National Resource  
113 Inventory, NRI database, USDA, 2000) and Europe, by deriving reference factors for soil  
114 erosion and for certain RUSLE parameters. They also introduced a procedure to scale slope,  
115 which is an important parameter in the topographical factors  $S$  and  $L$  of the RUSLE model. In  
116 this scaling procedure slope was scaled from the GTOPO30 1km resolution digital elevation  
117 model (USGS, 1996) to the coarser resolution of the erosion model based on high resolution OS  
118 Ordnance (10m resolution) and SRTM data on elevation (90m resolution, International Centre  
119 for Tropical Agriculture (CIAT), 2004) for England and Wales.

120 Doetterl et al. (2012) showed that together with the *S* factor, the rainfall erosivity or *R* factor  
121 explain up to 75 % of the erosion variability across agricultural areas at the large watershed  
122 scale, as these factors represent the triggers for soil erosion by providing energy for soil to erode.  
123 The *S* and *R* factors can also be seen as the natural components of the RUSLE model, as they  
124 have very little or no modification by human activities (Angulo-Martínez et al., 2009) apart from  
125 indirect effects on precipitation and extreme events due to anthropogenic climate change that are  
126 included in the *R* factor. In this way they represent the natural environmental constraints to soil  
127 erosion that are important to capture before the effect of human activities on soil erosion through  
128 land use change can be investigated. Previous studies on global soil erosion estimated the global  
129 *R* factor based on the total annual precipitation (Renard and Freimund, 1994), due to the lack of  
130 high resolution precipitation intensity on a global scale. However, high resolution precipitation  
131 intensity is an important explaining parameter of the *R* factor and therefore, the applicability of  
132 this method is limited.

133 The overall objective of this study is to extend the applicability of the RUSLE model to a coarse  
134 resolution at a global scale, in order to enable future studies on the effects of soil erosion for the  
135 past, current and future climate. To this end, we develop generally applicable methods that  
136 improve the estimation of slope and climatic factors from coarse resolution global datasets.  
137 These methods should not only be applicable across agricultural areas as in the studies of Van  
138 Oost et al. (2007) and Doetterl et al. (2012), but also across non-agricultural areas. We adjust the  
139 *S* factor to the coarse resolution of the global scale based on the scaling of slope according to the  
140 fractal method. The adjustment of the *R* factor to the global scale is based on globally applicable  
141 regression equations for different climate zones that include parameters for precipitation,  
142 elevation and the simple precipitation intensity. This approach is validated using several high  
143 resolution datasets on the *R* factor. Finally, the effects of these adjustments of both factors on  
144 global soil erosion rates are investigated separately and tested against independent estimates of  
145 soil erosion from high resolution and high precision datasets of Europe and the USA.

146

## 147 **2. Adjustment of the topographical factor**

### 148 **2.1 Scaling slope according to the fractal method**

149 The topographical factors of RUSLE are the slope steepness factor ( $S$ ) and a slope length factor  
 150 ( $L$ ). The  $S$  factor is generally computed by the continuous function of Nearing (1997):

$$151 \quad S = 1.5 + \frac{17}{1 + e^{(2.3 - 6.1 * \sin \theta)}} \quad (1)$$

152 And the  $L$  factor is computed according to Renard et al. (1997):

$$153 \quad L = \left(\frac{l}{22.13}\right)^m \quad (2)$$

$$154 \quad \text{where: } m = \frac{F}{1+F} \text{ and } F = \frac{(\sin \theta / 0.0896)}{(3 * (\sin \theta)^{0.8} + 0.56)} \quad (3)$$

155 in which  $\theta$  is the slope and  $l$  is the slope length in meters.

156 As seen in the equations of the  $L$  and  $S$  factors, slope is a crucial parameter and thus an accurate  
 157 estimation is essential in deriving accurate estimates of the  $L$  and  $S$  factors and finally also the  
 158 soil erosion rates. For an accurate estimation of slope the input elevation data from digital  
 159 elevation models (DEMs) should capture the detailed spatial variability in elevation. However,  
 160 global DEMs are often too coarse to capture the detailed topography because of the surface  
 161 smoothing effect. To account for this problem it is assumed that topography is fractal.  
 162 Following Klinkenberg and Goodchild (1992) and Zhang et al. (1999), slope can be expressed as  
 163 a function of the spatial scale by applying the variogram equation. The variogram equation is  
 164 used to approximate the fractal dimension of topography and is expressed as follows:

$$165 \quad (Z_p - Z_q)^2 = k d_{pq}^{A-2D} \quad (4)$$

166 so that:

$$167 \quad \frac{|Z_p - Z_q|}{d_{pq}} = \alpha d_{pq}^{1-D} \quad (5)$$

168 where  $Z_p$  and  $Z_q$  are the elevations at points  $p$  and  $q$ ,  $d_{pq}$  is the distance between  $p$  and  $q$ ,  $k$  is a  
 169 constant,  $\alpha = k^{0.5}$  and  $D$  is the fractal dimension. Because the left side of Eq. (5) represents the  
 170 slope, it can be assumed that the slope  $\theta$  is related to the spatial scale or the grid size  $d$  in:

$$171 \quad \theta = \alpha d^{1-D} \quad (6)$$

172 This result implies that by calculating the fractal properties ( $D$  and  $\alpha$ ) Eq. (6) can be used to  
 173 calculate slope at any specified scale  $d$ . The local fractal dimension describes the roughness of

174 the topography while the local value of  $\alpha$  is related to the concept of lacunarity, which is a  
175 measure of the size of “gaps” (valleys and plains) in the topography (Zhang et al., 2002). To  
176 estimate the spatial variations of the fractal dimension  $D$  and the fractal coefficient  $\alpha$ , Zhang et  
177 al. (1999) proposed to relate these parameters to the standard deviation of elevation. Hereby it is  
178 assumed that the standard deviation of elevation does not change much with the DEM resolution.  
179  $D$  is then calculated as a function of the standard deviation ( $\sigma$ ) in a 3 x 3 pixels moving window  
180 as proposed by Zhang et al. (1999):

$$181 \quad D = 1.13589 + 0.08452 \ln \sigma \quad (7)$$

182 To estimate  $\alpha$  we used the modified approach by Pradhan et al. (2006), who derived  $\alpha$  directly  
183 from the steepest slope in a 3 x 3 pixels moving window, called  $\alpha_{steepest}$  in the following. Having  
184 obtained  $\alpha_{steepest}$  and  $D$  from a grid at a given resolution, the scaled slope ( $\theta_{scaled}$ ) for a target grid  
185 resolution  $d_{scaled}$  is obtained by:

$$186 \quad \theta_{scaled} = \alpha_{steepest} d_{scaled}^{1-D} \quad (8)$$

187 Pradhan et al. (2006) also showed that in their case study the ideal target resolution for  
188 downscaling slope was 150m due the breakdown of the unifractal concept at very fine scales,  
189 which they showed to happen at a scale of 50m. Altogether, this fractal method shows that a high  
190 resolution slope can be obtained from a low resolution DEM as needed by the RUSLE model.

191

## 192 **2.2 Application of the fractal method on global scale**

193 In this study, we investigate the performance of the fractal method on a global scale using  
194 different global DEMs as a starting point. The target resolution of downscaling is put to 150m  
195 (about 5 arc-second) according to Pradhan et al. (2006). It should be noted that the original  
196 spatial scale that the RUSLE and USLE models are operating on is usually between 10 and  
197 100m, which indicates that the 150m target resolution may be still too coarse for a correct  
198 representation of slope. The DEMs that are used here are given in Table 1.

199 As reported in previous studies (Zhang et al., 1999; Chang and Tsai, 1991; Zhang and  
200 Montgomery, 1994), the average slope decreases with decreasing DEM resolution. This confirms  
201 the expectation of loss of detail in topography at lower DEM resolutions. A large difference is

### **Comment [VN2]:**

**Comment [4]: Reviewer #2:** why is a 3x3 pixel window chosen? Is it purely because this is the smallest moving window? What is the influence of this choice? Can changing window size in different topographical regions help?

**Reply:** As discussed in Zhang et al. (1999), a 3x3 pixel window is chosen mainly because of two reasons. First, it is the smallest moving window, secondly, it is assumed that the fractal coefficient  $\alpha$  and fractal dimension  $D$  are stable in this 3x3 pixel window. The last assumption is essential here, because the fractal method of scaling slope is mainly based on this assumption. If one would increase the moving window size, the fractal parameters could be less stable, independent of the topographical region. We already see that although we assume that in a 3x3 pixel window the fractal coefficients are stable, they actually change a little bit. This effect would increase with increasing moving window. Also, this effect is more pronounced in topographically complex regions.

202 found between the unscaled global average slope of the 5 arc-minute and the 30 arc-second  
203 DEMs, which is in the order of  $0.017 \text{ m m}^{-1}$  or 74 % (Table 2). After applying the fractal  
204 method, the scaled slopes of the DEMs at 150 m target resolution are all increased significantly  
205 compared to the unscaled slopes (Fig. 1). However, there is still a difference of about  $0.05 \text{ m m}^{-1}$   
206 or 8.5 % between the scaled slopes of the 5 arc-minute and the 30 arc-second DEMs (Table 2).  
207 This difference can be attributed to several factors. One factor could be the underlying  
208 assumption that the standard deviation of elevation ( $\sigma$ ) is independent of the DEM resolution.  
209 Although  $\sigma$  does not change much when considering different resolutions, there is still a general  
210 decrease in mean global  $\sigma$  when going from the 5 arc-minute to the 30 arc-second DEM (Table  
211 2). Due to the dependence of the fractal dimension  $D$  on  $\sigma$  (Zhang et al., 1999), a decrease of  $\sigma$   
212 leads to a decrease in  $D$  and therefore an increase in the scaled slope. Other factors that could  
213 play a role here are the dependence of  $\alpha_{steepest}$  on the steepest slope and the breakdown of the  
214 fractal method at certain scales and in certain environments. Zhang et al. (1999) mentioned that  
215 the scaling properties of slope are affected in very coarse resolution DEMs if  $\sigma$  changes  
216 considerably. On the other hand, Pradhan et al. (2006) mentioned the breakdown of the fractal  
217 method at very fine scales. This can indicate that the 150m target resolution is not appropriate for  
218 some topographically complex regions in the world when downscaling from the DEMs used in  
219 this study. Or based on the limitation of the fractal method as addressed by Zhang et al. (1999)  
220 the DEMs used in this study are too coarse to scale down the slope to 150m accurately.

221 After applying the fractal method on a 30 arc-second resolution DEM, the scaled slope shows a  
222 clear increase in detail, while the unscaled slope shows a strong smoothing effect (Fig. 2A and  
223 2B). It is found that after scaling the slope values range from 0 to 85 degrees and are less than 2  
224 degrees in 80% of the area. In contrast, all slope values are less than 45 degrees and range  
225 between 0 and 2 degrees in 89% of this area when slope is computed directly from the 30 arc-  
226 second DEM.

227 The scaled slope from the 30 arc-second DEM will be used in this study to estimate the global  
228 soil erosion rates by the RUSLE model.

229

### 230 **3. Adjustment of the rainfall erosivity factor**

231 **3.1 The approach by Renard and Freimund (1994)**

232 Rainfall erosivity ( $R$  factor) is described by Hudson (1971) and Wischmeier and Smith (1978) as  
233 the result of the transfer of the kinetic energy of raindrops to the soil surface. This causes a  
234 detachment of soil and the downslope transport of the soil particles depending on the amount of  
235 energy, rainfall intensity, soil type and cover, topography and management (Da Silva, 2004). The  
236 original method of calculating erosivity is described by Wischmeier and Smith (1978) and  
237 Renard et al. (1997) as:

238 
$$R = \frac{1}{n} * \sum_{j=1}^n \sum_{k=1}^{m_j} (EI_{30})_k \quad (9)$$

239 where  $n$  is the number of years of records,  $m_j$  is the number of storms of a given year  $j$ , and  $EI_{30}$   
240 is the rainfall erosivity index of a storm  $k$ . The event's rainfall erosivity index  $EI_{30}$  ( $\text{MJ mm ha}^{-1}$   
241  $\text{h}^{-1}$ ) is defined as:

242 
$$EI_{30} = I_{30} * \sum_{r=1}^m e_r v_r \quad (10)$$

243 where  $e_r$  and  $v_r$  are, respectively, the unit rainfall energy ( $\text{MJ ha}^{-1} \text{mm}^{-1}$ ) and the rainfall depth  
244 (mm) during a time period  $r$ , and  $I_{30}$  is the maximum rainfall intensity during a time period of 30  
245 minutes ( $\text{mm h}^{-1}$ ). The unit rainfall energy,  $e_r$ , is calculated for each time period as:

246 
$$e_r = 0.29 * (1 - 0.72 * e^{-0.05 * i_r}) \quad (11)$$

247 where  $i_r$  is the rainfall intensity during the time period ( $\text{mm h}^{-1}$ ).

248 The information needed to calculate the  $R$  factor according to the method of Wischmeier and  
249 Smith (1978) is difficult to obtain on a large spatial scale or in remote areas. Therefore, different  
250 studies have been done on deriving regression equations for the  $R$  factor (Angulo-Martinez et al.,  
251 2009, Meusburger et al., 2012, Goovaerts, 1999, Diodato and Bellocchi, 2010). Most of these  
252 studies, however, concentrate on a specific area and can therefore not be implemented on the  
253 global scale. Studies on global soil erosion estimation by the RUSLE model or a modified  
254 version of it (Doetterl et al., 2012, van Oost et al., 2007, Montgomery et al., 2007, Yang et al.,  
255 2003) have all used the method of Renard and Freimund (1994). Renard and Freimund related  
256 the  $R$  factor to the total annual precipitation based on erosivity data available for 155 stations in  
257 the USA, shown in the following equation:

258 
$$R = 0.0483 * P^{1.61}, \quad P \leq 850 \text{ mm}$$



259  $R=587.8-1.219*P+0.004105*P^2, \quad P > 850 \text{ mm}$  (12)

260 To test how this method performs globally, first the  $R$  factor was calculated in this study  
261 according to the method of Renard and Freimund (Eq. 12) using the 0.25 degree resolution  
262 annual precipitation data from the GPCC product (Table 1). Then, three regions were selected to  
263 validate the resulting  $R$  values and their variability: the USA (EPA, 2001), Switzerland  
264 (Meusburger et al., 2011), and the Ebro basin in Spain (Angulo-Martinez et al., 2009). For these  
265 regions high resolution erosivity data are available obtained from pluviographic data from local  
266 meteorological stations across the whole region.

267 Figure 3 shows that the  $R$  values computed with the Renard and Freimund method strongly  
268 overestimate  $R$  when compared to the high resolution  $R$  data of the selected regions. For the USA  
269 the  $R$  factor of Renard and Freimund shows an overall overestimation for western USA and for a  
270 large part of eastern USA when compared to the high resolution  $R$  (Table 76 and Fig. 3A).  
271 Especially a strong overestimation is seen for the north-west coast of the USA. This region is  
272 known to have complex rainfall patterns due to the presence of mountains and high local  
273 precipitation intensities with frequent snow fall (Cooper, 2011). It should be noted that the USA  
274 is not a completely suited case study for testing the  $R$  values computed with the Renard and  
275 Freimund method, as this method is based on data from stations in the USA. The available high  
276 resolution data on the  $R$  factor from Switzerland and the Ebro basin are better suited for an  
277 independent validation.

278 For Switzerland, which has a complex precipitation variability influenced by the relief of the  
279 Alps (Meusburger et al., 2012), the  $R$  factor of Renard and Freimund shows a strong overall  
280 overestimation when compared to the observed or high resolution  $R$  values (Table 76 and Fig.  
281 3B). For the Ebro basin located in Spain, the observed  $R$  data were available for the period 1997-  
282 2006 from Angulo-Martinez et al., 2009. Also here the method of Renard and Freimund  
283 overestimates the  $R$  factor and is not able to model the high spatial variability of the  $R$  data  
284 (Table 76 and Fig. 3C).

285

### 286 **3.2 The linear multiple regression approach using environmental factors**

287 To better represent the  $R$  factor on a global scale, the  $R$  estimation was based on the updated  
288 Köppen-Geiger climate classification (Table 3 and Fig. 4). The Köppen-Geiger climate  
289 classification is a globally climate classification and is based on the vegetation distribution  
290 connected to annual cycles of precipitation and temperature (Lohmann et al., 1993). The reason  
291 for this approach is that this classification system includes annual cycles of precipitation and is  
292 thus indirectly related to precipitation intensity. Based on this it is possible to derive regression  
293 equations for the  $R$  factor that are applicable for each individual climate zone. This provides a  
294 basis to calculate  $R$  with coarse resolution data on a globally scale.

295 As a basis for deriving the regression equations for the  $R$  factor for most climate zones the high  
296 resolution  $R$  maps of the USA from EPA (2001) were used. The USA covers most of the world's  
297 climate zones and is also the largest region with available high resolution  $R$  data. Linear multiple  
298 regression was used to adjust  $R$ :

$$299 \log(R_i) = \beta_0 + \sum_{j=1}^n \beta_{i_j} * \log(X_{i_j}) + \varepsilon_i, \text{ for } i = 1, 2, \dots, n \quad (13)$$

300 where  $X$  is the independent explanatory variable,  $j$  is the number of explanatory variables,  $\beta$  is a  
301 constant and  $\varepsilon$  is the residual.

302 The regression operates on one or more of the following parameters ( $X_j$ ): total annual  
303 precipitation (GPCC 0.25 degree product), mean elevation (ETOPO 5 DEM), and the simple  
304 precipitation intensity index, SDII. It should be mentioned that the SDII was only available on a  
305 very coarse resolution of 2.5 degree resolution for certain regions on earth, such as parts of  
306 Europe and the USA. The SDII is calculated as the daily precipitation amount on wet days ( $\geq 1$   
307 mm) in a certain time period divided by the number of wet days in that period. Previous studies  
308 that performed regression of  $R$  showed that precipitation and elevation were in most cases the  
309 only explanatory variables. Here, the SDII is added as it is a simple representation of  
310 precipitation intensity, which is an important explaining variable of  $R$ . The precipitation and  
311 SDII datasets were rescaled to a 5 arc-minute resolution (corresponding to 0.0833 degree  
312 resolution) to match the Köppen-Geiger climate classification data that was available at the  
313 resolution of 6 arc-minute (corresponding to 0.1 degree). Furthermore, high resolution erosivity  
314 data from Switzerland (Meusburger et al., 2011) and annual precipitation from the GPCC 0.5  
315 degree product were used to derive the regression equations for  $R$  for the polar (E) climates,  
316 which are not present in the USA. For the rest of the climate zones not present in the USA it was

**Comment [VN3]:**

**Comment [1]: Reviewer #1:** It seems that the two variables, annual precipitation and precipitation intensity, are not independent each other. Did you check independence among the variables used in the regression analysis?

**Reply:** We checked the independence of these variables and they are in some extent correlated, because the precipitation intensity is inferred from the long term total precipitation on wet days. We found an  $r$  squared of 0.5 when plotting the two variables against each other. However, these two variables contain different information. For example the precipitation intensity is shown to be crucial in a lot of climate zones (see for example the case of the Ebro basin in Spain). Also, the annual total precipitation provides additional information which makes the regression more accurate. Without the annual precipitation, the performance of the multiple regression approach is lower. So we decided that both variables play an important role in the multiple regression approach.

317 difficult to obtain high resolution erosivity data. Therefore, for those climate zones the method of  
318 Renard and Freimund was maintained to calculate erosivity. Also, if no clear improvement of the  
319 *R* factor is found when using the new regression equations for a specific climate zone, the *R*  
320 factor of Renard and Freimund is kept. Here, we mainly used the  $r^2$  combined with the residual  
321 standard error to evaluate if the new regression equations showed a clear improvement in the *R*  
322 factor. From the climate zones where high resolution erosivity data was available, the Renard  
323 and Freimund *R* factors were kept for the BWh and Csa climate zones. These are just two  
324 climate zones out of the 17 evaluated ones, which shows that the regression method performs  
325 better than the old method in most cases. All datasets for deriving the *R* factor are described in  
326 Table 1.

327

### 328 3.3 Application of the linear multiple regression method on a global scale

329 Tables 34 and 54 show the resulting regression equations for climate zones for which initially a  
330 low correlation was found between the *R* values calculated by the method of Renard and  
331 Freimund and the high resolution or observed *R* values from the maps of EPA (2001) and  
332 Meusburger et al. (2011). Figure 5 shows for each addressed climate zone how the method of  
333 Renard and Freimund and the new regression equations compare to the observed *R* of the USA.  
334 For the Ds climate zones the new regression equations showed only a slight improvement as  
335 compared to the method of Renard and Freimund. Also for the E climate zones the new  
336 regression equations still showed a significant bias. However, they performed much better  
337 compared to the method of Renard and Freimund. For most of the addressed climate zones the  
338 simple precipitation intensity index (SDII) explained a large part of the variability in the *R* factor.  
339 The elevation played a smaller role here. Elevation can be an important explaining variable in  
340 regions with a high elevation variability, which then affects the precipitation intensity.  
341 Furthermore, from Table 43 and Table 6 it can be concluded that the *R* factor in f climate zones,  
342 which have no dry season, can be easily explained by the total annual precipitation and the SDII.  
343 Dry climate zones, especially dry summer climate zones showed a weaker correlation, which is  
344 most probably due to the fact that the SDII is too coarse to explain the variability in the low  
345 precipitation intensity in the summer. It is also interesting to see that even though the SDII was  
346 derived from a very coarse dataset, it turned out to be still important for deriving more accurate *R*

#### Comment [VN4]:

Comment [8]: Reviewer #2: how is this evaluated? Using the  $r^2$ ? In how many cases are the Renard Freimund *R* factors kept?

Reply: Yes, we mainly used the  $r^2$  combined with the residual standard error to evaluate if the improvement of the *R* factor was significant. If the  $r^2$  value of the regression method was significantly different from the method of Renard and Freimund, then the regression method was preferred. In case there was not much difference in the  $r^2$  values between the methods, we looked at the differences in the residual standard error. In case of the E climates, the  $r^2$  was low for both methods, so we also compared the mean *R* values of these climates to the observed ones to see if there was improvement. The Renard and Freimund *R* factors are first of all kept for climate zones where we had no or too less high resolution data. From the climate zones where we had high resolution data, the Renard and Freimund *R* factors were kept for the BWh and Csa climates. These are just 2 climate zones out of 17. Although the Renard and Freimund method performed badly for the Csa climate, no improvement was found with the multiple regression approach. For the BWh the Renard and Freimund method performed slightly better than for the Csa climate, and the multiple regression approach did not change this result significantly. We highlight this here.

Formatted: Font: Italic

Formatted: Font: Italic

#### Comment [VN5]:

Comment [10]: Reviewer #2: should this be Table 5 rather than 3?

Reply: Table 3 and table 5 are now table 4 and table 6 in the revised manuscript. We can see the point you are making here. Both Table 4 and 6 show that the f climate zones can be explained by the total yearly precipitation and the SDII. Table 4 shows which the significant parameters are for the f climate zones, while table 6 shows that for these climate zones the regression performs well when compared to high resolution erosivity for the USA. We refer now to both tables here.

347 | values. Furthermore, Table 5-6 showed for each addressed climate zone a comparison of the  
348 | newly computed average  $R$  factor with the average observed  $R$  factor, and the uncertainty range.  
349 | The uncertainty range was computed by taking into account the standard deviation of each of the  
350 | parameters in the regression equations. As mentioned before, the E climate zones showed the  
351 | largest uncertainty range. The new regression equations significantly improved the  $R$  values and  
352 | spatial variability in the western USA and lead to a mean  $R$  factor that was closer to the data  
353 | mean (Table 6-7 and Fig. 6A). Although the new regression equations showed a bias for the E  
354 | climate zones (the minimum and maximum  $R$  were not captured), the resulting mean  $R$  for  
355 | Switzerland showed a strong improvement (Table 6-7 and Fig. 6B). Furthermore, the variability  
356 | in the estimated  $R$  compared well with the variability of the observed  $R$ . It should be noted that  
357 | Switzerland is not an independent case study anymore for the E climate zones. However, the  
358 | Ebro basin case study confirms that the improvement for the E climate zones that also occur  
359 | here, is significant (Fig. 6C). As the observed  $R$  values of the USA and Switzerland were used to  
360 | derive the regression equations, thea third case study, the Ebro basin in Spain, provided an  
361 | important independent validation. For the Ebro basin, the new regression equations not only  
362 | improved the overall mean but also captured the minimum  $R$  values better, resulting in an  
363 | improved representation of the  $R$  variability (Table 6-7 and Fig. 6C). In Fig. 6C, however, there  
364 | iwas a clear pattern separation in the newly computed  $R$  values, which was due to the fact that  
365 | the SDII data were not available for part of the Ebro basin. As mentioned before, SDII is an  
366 | important explaining parameter in the regression equations for most of the addressed climate  
367 | zones.

368 | Figure 7A showed the global patterns of the estimated  $R$  from respectively the method of Renard  
369 | and Freimund and the new regression equations. Figure 7B showed a difference plot between the  
370 | estimated  $R$  with the method of Renard and Freimund and the  $R$  estimated with the new  
371 | regression equations. The new regression equations significantly reduced the  $R$  values in most  
372 | regions. However, the tropical regions still showed unrealistic high  $R$  values (maximum  $R$  values  
373 | go up to  $1 * 10^5$  MJ mm ha<sup>-1</sup> h<sup>-1</sup> yr<sup>-1</sup>). This is because the  $R$  factor was not adjusted for the  
374 | tropical climate zones due to the lack of high resolution  $R$  data. Oliveira et al. (2012) found for  
375 | the  $R$  factor in Brazil that the maximum  $R$  values for the tropical climate zones reach 22,452 MJ  
376 | mm ha<sup>-1</sup> h<sup>-1</sup> yr<sup>-1</sup>.

**Comment [VN6]:**

**Comment [12]: Reviewer #2:**  
Figure 6 and text that refers to it, care should be taken to highlight that Switzerland is no longer a truly independent test given that this data has been used in the regressions. This doesn't invalidate the work, the improvements for Spain are impressive, but it should be discussed.

**Reply:** We mention in the revised manuscript about the fact that Switzerland is not an independent case study anymore after the regression. We also mention that in the Ebro basin in Spain the E climate zones, for which the  $R$  factor was adjusted in Switzerland, also occur. And there the improvement is also clearly visible.

**Formatted:** Font: (Default) Times New Roman, 12 pt

**Formatted:** Font: (Default) Times New Roman, 12 pt

377 Finally, it should be noted that the purpose of the adjusting methods in this study is to capture  
378 more accurately the large scale mean erosion rates rather than the extremes. Therefore, even  
379 though the new regression equations are still not accurate enough for certain climate zones, it is  
380 important that the mean *R* factor is represented well. The approach for adjusting the *R* factor also  
381 showed that even though there is no high temporal resolution precipitation intensity data  
382 available on a global scale, the *R* factor can still be represented well for most climate zones on a  
383 large spatial scale by using other parameters, such as elevation, and especially a representative of  
384 precipitation intensity, such as the SDII. The SDII played an important role here as it improved  
385 the estimation of the *R* factor significantly, even though data was only available at a very low  
386 resolution as compared to the other datasets of precipitation, elevation and climate zone  
387 classification.

388

## 389 **4 Global application of the adjusted RUSLE model**

### 390 **4.1 Computation of the soil erodibility and crop cover factors**

391 In the following the consequences of the new parameterizations of the *S* and *R* factors for global  
392 soil erosion rates are demonstrated. First, the other individual RUSLE factors, soil erodibility (*K*)  
393 and crop cover (*C*) needed to be computed. Estimations of the *K* factor were based on soil data  
394 from the gridded 30 arc-second Global Soil Dataset for use in Earth System Models (GSCE).  
395 GSCE is based on the Harmonized World Soil database (HWSD) and various other regional and  
396 national soil databases (Shangguan et al., 2014). The method of Torri et al. (1997) was then used  
397 to estimate the *K* factor. Volcanic soils were given a *K* factor of  $0.08 \text{ t ha h ha}^{-1} \text{ MJ}^{-1} \text{ mm}^{-1}$ , as  
398 these soil types are usually very vulnerable for soil erosion and the *K* values are beyond the  
399 range predicted by the method of Torri et al. (1997) (van der Knijff et al., 1999). To account for  
400 the effect of stoniness on soil erosion a combination of the methods used by Cerdan et al. (2010)  
401 and Doetterl et al. (2012) was applied, who base their methods on the original method of Poesen  
402 et al. (1994). For non-agricultural areas the method of Cerdan et al. (2010) was used where they  
403 reduced the total erosion by 30 % for areas with a gravel percentage larger or equal to 30%. For  
404 agricultural and grassland areas the method of Doetterl et al. (2012) was used, where erosion was  
405 reduced by 80 % in areas where the gravel percentage exceeded 12%.

406 The *C* factor was calculated according to the method of De Jong et al. (1998), using 0.25 degree  
407 Normalized Difference Vegetation Index (NDVI) and land use data for the year 2002. An  
408 important limitation of this method is the fact that in winter the *C* factor is estimated too large  
409 (van der Knijff et al., 1999). This is because the equation does not include the effects of mulch,  
410 decaying biomass and other surface cover reducing soil erosion. To prevent the *C* factor of being  
411 too large, maximum *C* values for forest and grassland of 0.01 and 0.05 for pasture were used.  
412 Doetterl et al. (2012) showed that the slope length (*L*) and support practice (*P*) factors do not  
413 contribute significantly to the variation in soil erosion at the continental scale ~~to global scale,~~  
414 ~~when compared to the contribution of the other RUSLE factors (S,R and C). However, this does~~  
415 ~~not mean that their influence on erosion should be ignored completely. They may play an~~  
416 ~~important role in local variation of erosion rates. In our erosion calculations we do not include~~  
417 ~~these factors, because we have too little to no data on these factors on a global scale. Including~~  
418 ~~them in the calculations would only add an additional large uncertainty to the erosion rates,~~  
419 ~~which would make it more difficult to judge the improvements we made to the S and R factors.-~~  
420 ~~Also, data on these factors are very scarce on global scale. Therefore it was decided not to~~  
421 ~~include these factors in the model.~~

422

#### 423 4.2 Computation of global soil erosion and comparison to empirical databases

424 The RUSLE model with the settings mentioned in the previous paragraph is applied on a 5 arc-  
425 minute resolution on a global scale for the present time period (see time resolutions of datasets in  
426 Table 1). Global soil erosion rates are calculated for four different versions of the RUSLE model:  
427 (a) the unadjusted RUSLE, (b) RUSLE with only an adjusted *S* factor, (c) RUSLE with only an  
428 adjusted *R* factor and (d) the adjusted RUSLE (all adjustments included). The global mean soil  
429 erosion rate for the adjusted RUSLE is found to be  $7 \text{ t ha}^{-1} \text{ y}^{-1}$  (Fig. 8A). When including the  
430 uncertainty arising from applying the linear multiple regression method, the mean global soil  
431 erosion rate differs between 6 and  $18 \text{ t ha}^{-1} \text{ y}^{-1}$ . Furthermore, the RUSLE version with only an  
432 adjusted *S* factor shows the highest mean global soil erosion rate, while the lowest rate is found  
433 for the RUSLE version with only the adjusted *R* factor (Table 78). From the global map showing  
434 the difference between the erosion rates of the S adjusted RUSLE and the unadjusted RUSLE  
435 versions (Fig. 8C) one can see that erosion rates are in general increased and mostly pronounced

#### Comment [VN7]:

Comment [2]: Reviewer #1: I have some concern about the statement that "... and support practice (P) factors do not contribute significantly to the variation in soil erosion at the continental scale." As you know, much efforts of soil management practice have been made to prevent erosion. In other words, I'm worrying about over-fitting in this study by putting too much focus on S and R factors.

Reply: We understand that this sentence may be misleading, management contributes a lot in preventing soil erosion in agricultural areas; however, the uncertainty in estimating the P factor due to the lack of data is large. Including this factor in the erosion estimations would mean including an additional large source of uncertainty. And as we want to keep the model simple and focus on presenting the improvements made to the S and R factors, we left this factor out of the calculations. We reformulate the sentence and add additional information explaining in a more detailed way like above why we ignored the L and P factors in our calculations.

Formatted: Font: (Default) Times New Roman, 12 pt

#### Comment [VN8]:

Comment [13]: Reviewer #2: I think it's important to provide mapped results for the erosion models as this is the end point for the work. Means do not tell the whole story and mapped output would help illustrate the discussion.

General comment: Reviewer #1: However, I have a suggestion that the global results should be presented and compared in a clearer manner. Currently, global erosion estimates were presented only in Table 7; no global map of erosion estimations were presented (only specific factors).

Reply: We did not present a global map of soil erosion rates, due to the fact that the other RUSLE factors (K, C and P) are not adjusted to the coarse resolution for global scale application as the S and R factors. We wanted to stress the improvements made by adjusting the S and R factors, rather than focusing on the final soil erosion rates. However, we agree that providing global maps of erosion rates can help making the statistics in table 8, in the revised manuscript, point out the improvements made in this study in a clearer way. So, additional to table 8, we will include 4 maps of global soil erosion rates. One map showing the erosion rates for the fully adjusted RUSLE model (Fig. 8A). The second map will show a difference plot between the fully adjusted and unadjusted RUSLE model (Fig. 8B). The third map will show a difference plot between the RUSLE model with only adjusted S factor and the unadjusted RUSLE model (Fig. 8C). And finally the last map will show a difference plot between the RUSLE model with only adjusted R factor and the unadjusted RUSLE model (Fig. 8D). These maps should highlight the different contributions of the ...

Formatted: Font: (Default) Times New Roman, 12 pt

436 in mountainous regions. This feature is ‘dampened’ by adjusting the R factor. Looking at the  
437 global map showing the difference between the R adjusted RUSLE and unadjusted RUSLE  
438 versions (Fig. 8D), one can see that the erosion rates are overall decreased in regions where the  
439 adjustments are made. When combining both adjustments of the RUSLE model in the fully  
440 adjusted RUSLE version and subtract the unadjusted RUSLE erosion rates (Fig. 8B), one can see  
441 that the erosion rates are slightly decreased in areas where the R factor is adjusted. However, in  
442 the tropics for example there is an increase in erosion rates by the fully adjusted RUSLE due to  
443 the lack of adjusting the R factor there. This indicates that these two factors balance each other,  
444 and that it is important to have a correct representation of all the RUSLE factors on a global scale  
445 in order to predict reliable erosion rates. This indicates that these two factors balance each other,  
446 and that it is important to have a correct representation of all the RUSLE factors on a global scale  
447 in order to predict reliable erosion rates.

448 In this study the *K* and *C* factors are not tested and adjusted for a coarse resolution at the global  
449 scale and thus validation with existing empirical databases on soil erosion is not fully justified.  
450 However, to test if the global erosion rates are in an acceptable range, they are compared to  
451 erosion estimates from the NRI database for the USA and erosion estimates from the study of  
452 Cerdan et al. (2010) for Europe. These are to our knowledge the only large scale high resolution  
453 empirical databases on soil erosion.

454 The NRI database contains USLE erosion estimates for the year 1997, which are available at the  
455 HUC4 watershed level. After aggregating the resulting erosion rates from the adjusted and  
456 unadjusted RUSLE models to the HUC4 watershed level, the results showed that the mean  
457 erosion rates from the adjusted RUSLE model come closer to that of the NRI database (Table 8-9  
458 and Fig. 98A). However, the maximum observed mean HUC4 soil erosion rate from the adjusted  
459 RUSLE was twice as high as compared to the NRI database. This maximum is observed in the  
460 hilly and relatively wet region on the west coast of the USA. From these results we can conclude  
461 that the erosion rates of the adjusted RUSLE fall in the range of observed values, but that there  
462 are still some local overestimations. For example, the north west of the US shows a slightly  
463 worse performance in the adjusted model most probably because in this region the estimation of  
464 the *R* factor could not be improved, while the *S* factor is increased. This gives an overall increase  
465 in soil erosion rates. In this region of the USA, the Csb climate prevails, for which the *R* factor is

**Comment [VN9]:**

**Comment [14]:** Reviewer #2: What’s happened in the north west of the US with the adjusted model? Perhaps the authors can comment.

**Reply:** See added explanation in text

**Formatted:** Font: (Default) Times New Roman, 12 pt

**Formatted:** Font: (Default) Times New Roman, 12 pt, Italic

**Formatted:** Font: (Default) Times New Roman, 12 pt

**Formatted:** Font: (Default) Times New Roman, 12 pt, Italic

**Formatted:** Font: (Default) Times New Roman, 12 pt

**Formatted:** Font: (Default) Times New Roman, 12 pt, Italic

**Formatted:** Font: (Default) Times New Roman, 12 pt

466 still difficult to estimate in a correct way (Table 4). So for this climate there are some outliers in  
467 the  $R$  factor in this specific region.

**Formatted:** Font: (Default) Times New Roman, 12 pt

**Formatted:** Font: (Default) Times New Roman, 12 pt, *Italic*

**Formatted:** Font: (Default) Times New Roman, 12 pt

468 For Europe, Cerdan et al. (2010) used an extensive database of measured erosion rates on plots  
469 under natural rainfall. They extrapolated measured erosion rates to the whole Europe (European  
470 Union area) and adjusted them with a topographic correction based on the  $L$  and  $S$  factors of  
471 RUSLE, and a correction to account for soil stoniness. For comparison, the soil erosion rates  
472 from Cerdan et al. (2010) and the RUSLE estimates are aggregated at country level. The  
473 performance of the adjusted RUSLE model was not as good for Europe compared to the USA,  
474 which is not surprising due to the fact that the RUSLE model is based on soil erosion data of the  
475 USA. However, also on the European scale the adjusted RUSLE model performed better than the  
476 unadjusted RUSLE model (Table 8-9 and Fig. 9B). Especially the large erosion rates in the  
477 south of Europe as observed in the results of the unadjusted RUSLE model are less extreme for  
478 the adjusted RUSLE model results. Still, the overall mean erosion rate for Europe was  
479 overestimated by approximately two times (Table 89).

480 These biases in erosion rates as seen for the USA and Europe can be attributed to several factors.  
481 Firstly, the other RUSLE factors ( $K$  and  $C$ ) and the way they interact with each other are not  
482 adjusted to the coarse resolution of the global scale. From figures 8, which provide global  
483 erosion rates, no clear signal can be found for which land cover types the RUSLE performs  
484 worse or better. In general, we can see that the adjusted RUSLE model still overestimates  
485 erosion rates for most land cover types. A short analysis for Europe showed that the largest  
486 biases are found for shrubs, and the least for grassland. However, a more explicit analysis is  
487 needed here to find out how we can improve the contribution of land cover and land use to  
488 erosion rates in the RUSLE model. For example looking at the location of land use in a certain  
489 grid cell could make a difference in the resulting erosion rates. For example, a possible effect  
490 that is usually not captured by the RUSLE model is the location of land use in a certain gridcell.

**Comment [VN10]:**

**Comment [16]: Reviewer #2:** Can you say something more definitive here? You can see where the model is overestimating, and you know the  $K$  and  $C$  factors for these areas - are there trends here, i.e. is it systematically overestimating in regions dominated by arable land covers?

**Reply:** We shortly took a look at how the adjusted RUSLE model performs for different land cover types in the USA and Europe and didn't see a clear signal where the RUSLE performs worse and where better. The global maps on erosion rates from the new figures can provide some insight here as they can make the analysis spatially explicit. In general, we see that the adjusted RUSLE model still overestimates erosion rates for most land cover types. However, when taking a more accurate look the largest biases are found for shrubs, and the least for grassland. A lot of factors play a role here, for example it is important to consider where the land use is allocated. On steep hillslopes the effect on erosion would be different than in flat areas. So a more explicit analysis is needed here to find out how we can improve the contribution of land cover and land use to erosion rates in the RUSLE model. We add this explanation in the text.

**Formatted:** Font: (Default) Times New Roman, 12 pt

**Formatted:** Font: (Default) Times New Roman, 12 pt

491 If the land use in a grid cell is located on steep slopes the resulting erosion in that gridcell would  
492 be higher than when it would be located in the flatter areas. In this study, however, only mean  
493 fractions of land cover and the NDVI are used for each gridcell, which can lead to possible  
494 biases in the resulting erosion rates. Secondly, land management is not accounted for in this  
495 study, which could introduce an important systematic bias in the soil erosion rates for especially  
496 agricultural areas. Furthermore, uncertainties in the coarse resolution land cover/land use, soil



497 and precipitation datasets that are not accounted for, can lead to the model biases. Also, better  
498 adjustment of the  $R$  factor for climate zones such as the E climate zones, could help improving  
499 the overall results. Some biases in the erosion rates can also be attributed to the fact that stepped  
500 relief, where flat plateaus are separated by steep slopes, are not well captured by the 150m target  
501 resolution used in the fractal method to scale slope. In this way erosion would be overestimated  
502 in these areas. Finally, errors and limitations in the observational datasets can also contribute to  
503 the differences between model and observations. The study of Cerdan et al. (2010) on Europe for  
504 example used extrapolation of local erosion data to larger areas that could introduce some biases.  
505 Also the underlying studies on measured erosion rates used different erosion measuring  
506 techniques that can be linked to different observational errors.

507

## 508 **5 Conclusions**

509 In this study we introduced specific methods to adjust the topographical and rainfall erosivity  
510 factors to improve the application of the RUSLE model on a global scale using coarse resolution  
511 input data.

512 Our results show that the fractal method by Zhang et al. (1999) and Pradhan et al. (2006) can be  
513 applied on coarse resolution DEMs to improve the resulting slope. Although the slope  
514 representation improved after applying this method, the results still show a slight dependence on  
515 the original grid resolution. This is attributable to several factors such as the underlying  
516 assumption that the standard deviation of elevation ( $\sigma$ ) is independent of the DEM resolution,  
517 and to the breakdown of the fractal method at certain scales.

518 We compared the rainfall erosivity calculated by the method of Renard and Freimund to  
519 available high resolution or observed erosivity data of the USA, Switzerland and the Ebro basin,  
520 and showed overall significant biases. We implemented a linear multiple regression method to  
521 adjust erosivity for climate zones of the Köppen-Geiger climate classification system in the USA  
522 that showed a bias in erosivity calculated with the method of Renard and Freimund. Using  
523 precipitation, elevation and the simple precipitation intensity index as explaining parameters, the  
524 resulting adjusted erosivity compares much better to the observed erosivity data for the USA,  
525 Switzerland and the Ebro basin. Not only the mean values but also the spatial variability in  
526 erosivity is improved. It was surprising to notice that using the rather coarse resolution simple

527 precipitation intensity index in the regression analysis made it possible to explain much of the  
528 variability in erosivity. This, once more, underpins the importance of precipitation intensity in  
529 erosivity estimation.

530 After calculating the newly adjusted erosivity on a global scale, it is apparent that the tropical  
531 climate zones, for which erosivity was not adjusted, show strong overestimations in some areas  
532 when compared to estimated erosivity from previous studies. This shows that adjusting erosivity  
533 for the tropical climate zones should be the next step. The challenge is to find enough reliable  
534 long term and high resolution erosivity data for those regions.

535 To investigate how the adjusted topographical and rainfall erosivity factors affect the global soil  
536 erosion rates, we applied the adjusted RUSLE model on a global scale and estimate a mean  
537 global soil erosion rate of  $7 \text{ t ha}^{-1} \text{ y}^{-1}$ . It is, however, difficult to provide accurate uncertainty  
538 estimates to the global erosion rates of this study and to provide a good validation with  
539 observations, due to lack of high resolution data on other individual RUSLE factors such as the  
540 soil erodibility, slope length and support practice. These RUSLE factors, together with the crop  
541 cover factor, which includes the effects of land use, are therefore not adjusted for application on  
542 a coarse resolution on global scale.

543 To test if the soil erosion rates from the adjusted RUSLE model are in a realistic range, we  
544 compared the results to the USLE erosion estimates for the USA from the NRI database and the  
545 erosion estimates for Europe from the study of Cerdan et al. (2010). The adjusted RUSLE soil  
546 erosion rates, which we aggregated to the HUC4 watershed level, show a better comparison with  
547 the NRI USLE estimates for the USA than the unadjusted RUSLE erosion rates. For Europe the  
548 comparison of the adjusted RUSLE soil erosion rates to the study of Cerdan et al. (2010) were  
549 not as good as for the USA. This is not surprising due to the fact that the parameterizations of the  
550 RUSLE model are based on soil erosion data of the USA. However, also for Europe, the adjusted  
551 RUSLE model performs better than the unadjusted RUSLE model.

552 We find strong overestimations by the adjusted RUSLE model for hilly regions in the west coast  
553 of the USA and for south of Europe. We argue that besides for reasons mentioned before, these  
554 biases are due to the fact that the topographical detail may not be enough in some regions to  
555 capture the true variability in soil erosion effects by topography. Also erosivity could not be

556 adjusted for some climate zones that are not present in the USA or Switzerland, and needs to be  
557 improved for climate zones such as the polar climate zones.

558 We conclude that even though there is still much improvement of the RUSLE model possible  
559 with respect to topography and erosivity, the methods proposed in this study seem to be  
560 promising tools for improving the global applicability of the RUSLE model. A globally  
561 applicable version of the RUSLE model together with data on environmental factors from Earth  
562 System Models (ESMs) can provide the possibility for future studies to estimate accurate soil  
563 erosion rates for the past, current and future time periods.

564

#### 565 **Acknowledgements**

566

567 We like to thank the anonymous reviewers for their useful comments. The article processing  
568 charges for this open-access publication have been covered by the Max Planck Society.

569 **References**

- 570 1 Amante, C. and Eakins, B. W.: ETOPO1 1 Arc-Minute Global Relief Model: Procedures,  
571 Data Sources and Analysis, NOAA Technical Memorandum NESDIS NGDC-24,  
572 National Geophysical Data Center, NOAA, 2009.
- 573 2 Angulo-Martínez, M., López-Vicente, M., Vicente-Serrano, S. M. and Beguería, S.:  
574 Mapping rainfall erosivity at a regional scale: a comparison of interpolation methods in  
575 the Ebro Basin (NE Spain), *J. Hydrol. Earth Syst. Sc.*, 13, 1907-1920, 2009,  
576 <http://www.hydrol-earth-syst-sci.net/13/1907/2009/>.
- 577 3 Bork, H. R. and Lang A.: Quantification of past soil erosion and land use / land cover  
578 changes in Germany, in: Long term hillslope and fluvial system modelling. Concepts and  
579 case studies from the Rhine river catchment, *Lecture Notes in Earth Sc.*, 101, 231-239,  
580 2003.
- 581 4 Cerdan, O., Govers, G., Le Bissonnais, Y., Van Oost, K., Poesen, J., Saby, N., Gobin, a.,  
582 Vacca, a., Quinton, J., Auerswald, K., Klik, a., Kwaad, F. J. P. M., Raclot, D., Ionita, I.,  
583 Rejman, J., Rousseva, S., Muxart, T., Roxo, M. J. and Dostal, T.: Rates and spatial  
584 variations of soil erosion in Europe: A study based on erosion plot data, *Geomorphology*,  
585 122(1-2), 167–177, doi:10.1016/j.geomorph.2010.06.011, 2010.
- 586 5 Chang, K. T. and Tsai, B. W.: The effect of DEM resolution on slope and aspect  
587 mapping, *Cartography and Geographic Information Systems*, 18(1), 69-77, 1991.
- 588 6 Cooper K.: Evaluation of the Relationship between the RUSLE R-Factor and Mean  
589 Annual Precipitation, available at:  
590 [http://www.engr.colostate.edu/~pierre/ce\\_old/Projects/linkfiles/Cooper%20R-factor-](http://www.engr.colostate.edu/~pierre/ce_old/Projects/linkfiles/Cooper%20R-factor-Final.pdf)  
591 [Final.pdf](http://www.engr.colostate.edu/~pierre/ce_old/Projects/linkfiles/Cooper%20R-factor-Final.pdf) (last access: 15 January 2015), 2011.
- 592 7 Da Silva, A. M.: Rainfall erosivity map for Brazil, *Catena*, 57(3), 251–259,  
593 doi:10.1016/j.catena.2012.08.006, 2004.
- 594 8 De Jong, S. M., Brouwer, L. C. and Riezebos, H. Th.: Erosion hazard assessment in the  
595 Peyne catchment, France, Working paper DeMon-2 Project, Dept. Physical Geography,  
596 Utrecht University, 1998.

- 597 9 Diodato, N. and Bellocchi, G.: MedREM, a rainfall erosivity model for the  
598 Mediterranean region, *J. Hydrol.*, 387(1-2), 119–127, doi:10.1016/j.jhydrol.2010.04.003,  
599 2010.
- 600 10 Doetterl, S., Van Oost, K. and Six, J.: Towards constraining the magnitude of global  
601 agricultural sediment and soil organic carbon fluxes, *Earth Surf. Process. Landforms*,  
602 37(6), 642–655, doi: 10.1002/esp.3198, 2012.
- 603 11 Donat, M. G., Alexander, L.V., Yang, H., Durre, I., Vose, R. and Caesar, J.: Global  
604 Land-Based Datasets for Monitoring Climatic Extremes, *Bulletin American*  
605 *Meteorological Society*, 94, 997–1006, 2013.
- 606 12 Friedl, M. A., Strahler, A. H. and Hodges, J.: ISLSCP II MODIS (Collection 4) IGBP  
607 Land Cover, 2000-2001. In Hall, Forest G., G. Collatz, B. Meeson, S. Los, E. Brown de  
608 Colstoun, and D. Landis (eds.), *ISLSCP Initiative II Collection*, edited by: Hall, F. G.,  
609 Collatz, G., Meeson, B., Los, S., Brown de Colstoun, E., and Landis, D., from Oak Ridge  
610 National Laboratory Distributed Active Archive Center, Oak Ridge, Tennessee, U.S.A.,  
611 available online at: <http://daac.ornl.gov/> (last access: 15 January 2015), 2010.
- 612 13 Gesch, D.B., Verdin, K.L. and Greenlee, S.K.: New land surface digital elevation model  
613 covers the earth, *Eos, Transactions, AGU*, 80(6), 69–70, doi: 10.1029/99EO00050, 1999.
- 614 14 Goll, D. S., Brovkin, V., Parida, B. R., Reick, C. H., Kattge, J., Reich, P. B., van  
615 Bodegom, P. M. and Niinemets, Ü.: Nutrient limitation reduces land carbon uptake in  
616 simulations with a model of combined carbon, nitrogen and phosphorus cycling,  
617 *Biogeosciences*, 9, 3547–3569, doi:10.5194/bg-9-3547-2012, 2012.
- 618 15 Goovaerts, P.: Using elevation to aid the geostatistical mapping of rainfall erosivity,  
619 *Catena*, 34, 227–242, doi:10.1016/S0341-8162(98)00116-7, 1999.
- 620 16 Gruber, N. and Galloway, J. N.: An Earth-system perspective of the global nitrogen  
621 cycle., *Nature*, 451, 293–6, doi:10.1038/nature06592, 2008.
- 622 17 Hall, F. G., Brown de Colstoun, E., Collatz, G. J., Landis, D., Dirmeyer, P., Betts, A.,  
623 Huffman, G. J., Bounoua, L. and Meeson, B.: ISLSCP Initiative II global data sets:  
624 Surface boundary conditions and atmospheric forcings for land-atmosphere studies, *J.*  
625 *Geophys. Res.*, 111, D22S01, doi:10.1029/2006JD007366, 2006.

- 626 18 Hooke, R. L.: On the history of humans as geomorphic agents, *Geology*, 28, 843–846,  
627 doi:10.1130/0091-7613(2000)28<843:OTHOHA>2.0.CO;2, 2000.
- 628 19 Hudson N.: *Soil Conservation*, Cornell University Press, Ithaca, 1971.
- 629 20 Ito, A.: Simulated impacts of climate and land-cover change on soil erosion and  
630 implication for the carbon cycle, 1901 to 2100, *Geophys. Res. Lett.*, 34, L09403,  
631 doi:10.1029/2007GL029342, 2007.
- 632 21 Klinkenberg, B. and Goodchild, M. F.: The fractal properties of topography: A  
633 comparison of methods, *Earth Surf. Process. Landforms*, 17, 217-234,  
634 doi:10.1002/esp.3290170303, 1992.
- 635 22 Lal, R.: Soil erosion and the global carbon budget, *Environ. Int.*, 29, 437–50,  
636 doi:10.1016/S0160-4120(02)00192-7, 2003.
- 637 23 Lohmann, U., Sausen, R., Bengtsson, L., Cubasch, U., Perlwitz, J. and Roeckner, E.: The  
638 Köppen climate classification as a diagnostic tool for general circulation models, *Climate*  
639 *Res.*, 3, 177-193, 1993.
- 640 24 Meusburger, K., Steel, a., Panagos, P., Montanarella, L. and Alewell, C.: Spatial and  
641 temporal variability of rainfall erosivity factor for Switzerland, *Hydrol. Earth Syst. Sci.*  
642 *Discuss.*, 8, 8291–8314, doi:10.5194/hessd-8-8291-2011, 2011.
- 643 25 Meusburger, K., Steel, a., Panagos, P., Montanarella, L. and Alewell, C.: Spatial and  
644 temporal variability of rainfall erosivity factor for Switzerland, *Hydrol. Earth Syst. Sci.*,  
645 16, 167–177, doi:10.5194/hess-16-167-2012, 2012.
- 646 26 Meyer-Christoffer, A., Becker, A., Finger, P., Rudolf, B., Schneider, U. and Ziese, M.:  
647 GPCP Climatology Version 2011 at 0.25°: Monthly Land-Surface Precipitation  
648 Climatology for Every Month and the Total Year from Rain-Gauges built on GTS-based  
649 and Historic Data, 2011.
- 650 27 Milliman, J. D. and Syvitski, J. P. M.: Geomorphic / Tectonic Control of Sediment  
651 Discharge to the Ocean : The Importance of Small Mountainous Rivers, *J. Geology*, 100,  
652 525–544, 2014.

- 653 28 Montgomery, D. R.: Soil erosion and agricultural sustainability, *PNAS*, 104, 13268–  
654 13272, doi: 10.1073/pnas.0611508104, 2007.
- 655 29 National Geophysical Data Center/NESDIS/NOAA/U.S. Department of Commerce:  
656 TerrainBase, Global 5 Arc-minute Ocean Depth and Land Elevation from the US  
657 National Geophysical Data Center (NGDC), Research Data Archive at the National  
658 Center for Atmospheric Research, Computational and Information Systems Laboratory,  
659 available online at: <http://rda.ucar.edu/datasets/ds759.2/> (last access 30 November 2014),  
660 1995.
- 661 30 Nearing, M.A.: A single, continues function for slope steepness influence on soil loss,  
662 *Soil. Sci. Soc. Am. J.*, 61: 917-929, doi:10.2136/sssaj1997.03615995006100030029x,  
663 1997.
- 664 31 Oliveira, P. T. S., Wendland, E. and Nearing, M. A.: Rainfall erosivity in Brazil: A  
665 review, *Catena*, 100, 139–147, doi:10.1016/j.catena.2012.08.006, 2013.
- 666 32 Peel, M. C., Finlayson, B. L. and McMahon, T. A.: Updated world map of the Köppen-  
667 Geiger climate classification, *HESS*, 1633–1644, 2007.
- 668 33 Pimentel, D., Harvey, C., Resosudarmo, P., Sinclair, K., Kurz, D., McNair, M., Cris, S.,  
669 Shpritz, L., Fitton, L., Saffouri, R. and Blair, R.: Environmental and economic costs of  
670 soil erosion and conservation benefits, *Science*, 267, 1117-1123, 1995.
- 671 34 Poesen, J., Nachtergaele, J., Verstraeten, G. and Valentin, C.: Gully erosion and  
672 environmental change: importance and research needs, *Catena*, 50, 91–133,  
673 doi:10.1016/S0341-8162(02)00143-1, 2003.
- 674 35 Pradhan, N. R., Tachikawa, Y. and Takara, K.: A downscaling method of topographic  
675 index distribution for matching the scales of model application and parameter  
676 identification, *Hydrol. Process.*, 20, 1385–1405, doi:10.1002/hyp.6098, 2006.
- 677 36 Quinton, J. N., Govers, G., Van Oost, K. and Bardgett, R. D.: The impact of agricultural  
678 soil erosion on biogeochemical cycling, *Nat. Geosci.*, 3, 311–314, doi:10.1038/ngeo838,  
679 2010.
- 680 37 Regnier, P., Friedlingstein, P., Ciais, P., Mackenzie, F. T., Gruber, N., Janssens, I. A.,  
681 Laruelle, G. G., Lauerwald, R., Luysaert, S., Andersson, A. J., Arndt, S., Arnosti, C.,

682 Borges, A. V., Dale, A. W., Gallego-Sala, A., Godd ris, Y., Goossens, N., Hartmann, J.,  
683 Heinze, C., Ilyina, T., Joos, F., LaRowe, D. E., Leifeld, J., Meysman, F. J. R., Munhoven,  
684 G., Raymond, P. a., Spahni, R., Suntharalingam, P. and Thullner, M.: Anthropogenic  
685 perturbation of the carbon fluxes from land to ocean, *Nat. Geosci.*, 6(8), 597–607,  
686 doi:10.1038/ngeo1830, 2013.

687 38 Reich, P. B. and Hungate, B. A.: Carbon-Nitrogen in Terrestrial Interactions in Response  
688 Ecosystems to Rising Atmospheric Carbon Dioxide, *Annu. Rev. Ecol. Evol. Syst.*, 37,  
689 611–636, doi:10.2307/annurev.ecolsys.37.091305.30000023, 2006.

690 39 Renard, K. G. and Freimund, J. R.: Using monthly precipitation data to estimate the R-  
691 Factor in the revised USLE, *J. Hydrol.*, 157, 287-306, doi:10.1016/0022-1694(94)90110-  
692 4, 1994.

693 40 Renard, K. G., Foster, G. R., Weesies, G.A., Mccool, D. K. and Yoder, D. C.: Predicting  
694 Soil Erosion by Water: a Guide to Conservation Planning with the Revised Universal Soil  
695 Loss Equation (RUSLE), *Agriculture Handbook 703*, USDA, 1997.

696 41 Schneider, U., Becker, A., Finger, P., Meyer-Christoffer, A., Rudolf, B. and Ziese, M.:  
697 GPCP Full Data Reanalysis Version 6.0 at 0.5 : Monthly Land-Surface Precipitation  
698 from Rain-Gauges built on GTS-based and Historic Data, 2011.

699 42 Shangguan, W., Dai, Y., Duan, Q., Liu, B. and Yuan, H.: A Global Soil Data Set for  
700 Earth System Modeling, *J. Adv. Model. Earth Syst.*, 6, 249-263, doi:  
701 10.1002/2013MS000293, 2014.

702 43 Stallard, R. F.: Terrestrial sedimentation and the carbon cycle: Coupling weathering and  
703 erosion to carbon burial, *Global Geochem. Cy.*, 12, 231–257, doi:10.1029/98GB00741,  
704 1998.

705 44 Thornton, P. E., Lamarque, J.-F., Rosenbloom, N. a. and Mahowald, N. M.: Influence of  
706 carbon-nitrogen cycle coupling on land model response to CO 2 fertilization and climate  
707 variability, *Global Biogeochem. Cycles*, 21, n/a–n/a, doi:10.1029/2006GB002868, 2007.  
708

**Formatted:** Left, Indent: Left: 0", Hanging: 0.5", Space Before: 6 pt, After: 0 pt, Line spacing: 1.5 lines

**Formatted:** Font: (Default) Times New Roman, 12 pt

**Formatted:** Justified, Space Before: 0 pt



709 | 45 Torri, D., Poesen, J. and Borselli, L.: Predictability and uncertainty of the soil erodibility  
710 factor using a global dataset, *Catena*, 31, 1-22, doi:10.1016/S0341-8162(97)00036-2,  
711 1997.

712 46 Tucker, C., Pinzon, J., Brown, M., Slayback, D., Pak, E., Mahoney, R., Vermote, E. and  
713 El Saleous, N.: An extended AVHRR 8-km NDVI dataset compatible with MODIS and  
714 SPOT vegetation NDVI data, *Int. J. Remote Sens.*, 26, 4485–4498, 2005.

715 47 United Nations Convention to Combat Desertification (UNCCD): Zero Net Land  
716 Degradation, 2012.

717 48 United States Environmental Protection Agency: Stormwater Phase 2 Final Rule,  
718 Construction Rainfall Erosivity Waiver, EPA 833-F-00-014, 2001.

719 49 US Department of Agriculture: Summary Report: 1997 National Resources Inventory  
720 (revised December 2000), Natural Resources Conservation Service, Washington, DC,  
721 and Statistical Laboratory, Iowa State University, Ames, Iowa, 2000.

722 50 US Department of Commerce, National Oceanic and Atmospheric Adminis.: 2-minute  
723 Gridded Global Relief Data (ETOPO2), 2001.

724 51 US Geological Survey.: GTOPO30 Arc-Second Elevation Data Set, EROS Data Center  
725 (EDC) Distributed Active Archive Center (DAAC), Sioux Falls, available online at:  
726 <http://edcdaac.usgs.gov/gtopo30/gtopo30.html> (last access 15 January 2015), 1996.

727 52 Van der Knijff, J. M., Jones, R. J. A. and Montanarella, L.: Soil Erosion Risk Assessment  
728 in Italy, Joint Research Center, EUR19022EN, European Commission, 1999.

729 53 Van Oost, K., Quine, T. a, Govers, G., De Gryze, S., Six, J., Harden, J. W., Ritchie, J. C.,  
730 McCarty, G. W., Heckrath, G., Kosmas, C., Giraldez, J. V, da Silva, J. R. M. and  
731 Merckx, R.: The impact of agricultural soil erosion on the global carbon cycle, *Science*,  
732 318(5850), 626–9, doi:10.1126/science.1145724, 2007.

733 54 Wilkinson, B. H. and McElroy, B. J.: The impact of humans on continental erosion and  
734 sedimentation, *Geol. Soc. Am. Bull.*, 119, 140–156, doi:10.1130/B25899.1, 2007.

735 55 Wischmeier, W. H. and Smith, D. D.: Predicting Rainfall Erosion Losses. A guide to  
736 conservation planning, *Agricultural Handbook 537*, USDA, Washington, 58 pp, 1978.

- 737 56 Yang, D., Kanae, S., Oki, T., Koike, T. and Musiaka, K.: Global potential soil erosion  
738 with reference to land use and climate changes, *Hydrol. Process.*, 17, 2913–2928,  
739 doi:10.1002/hyp.1441, 2003.
- 740 57 Zhang, W. and Montgomery, D. R.: Digital elevation model grid size, landscape  
741 representation, and hydrologic simulations, *Water Resour. Res.*, 30, 1019-1028,  
742 doi:10.1029/93WR03553, 1994.
- 743 58 Zhang, X., Drake, N. and Wainwright, J.: Scaling land surface parameters for global-  
744 scale soil erosion estimation, *Water Resour. Res.*, 38, 19–1–19–9,  
745 doi:10.1029/2001WR000356, 2002.
- 746

Table 1. List of datasets used in this study

Category	Dataset	Source	Spatial resolution	<del>Temporal-</del> <del>period</del> <del>resolution</del>	Variables
DEM	GTOPO Elevation Model	USGS, 1996, Gesch et al., 1999	30 arc-seconds		elevation
	ETOPO1 Elevation Model	Amante and Eakins, 2009	1 arc-minute		elevation
	ETOPO2 Elevation Model	US Department of Commerce and NOAA, 2001	2 arc-minute		elevation
	ETOPO5 Elevation Model	National Geophysical Data Center/NESDIS/NOAA, 1995	5 arc-minute		elevation
Climate	GPCC 0.5 degree dataset	Schneider et al., 2011	0.5 degrees	Years 1989- 2010	total yearly precipitation

**Comment [VN11]:**

**Comment [4]: Reviewer #1:** The column "Temporal resolution" does not provide temporal resolution (e.g., daily, monthly, annual) but show only temporal period. Please correct the label or data in the column.

**Reply:** Changed accordingly

	GPCC 0.25 degree dataset	Meyer-Christoffer et al., 2011	0.25 degrees	years 1951-2000	total yearly precipitation
	GHCNDEX dataset	CLIMDEX (Donat et al., 2013)	2.5 degrees	years 1951-present	simple precipitation intensity index (SDII)
	Köppen-Geiger dataset	Peel et al., 2007	5 arc-minute		Köppen-Geiger climate classifications
Soil	Global Soil Dataset for use in Earth System Models (GSCE)	Shangguan et al., 2014	30 arc-seconds		sand, silt and clay fractions, organic matter %, gravel %
	Harmonized World Soil Database (HWSD) version 1.2	Nachtergaele et al., 2012	30 arc-seconds		volcanic soils
Land-cover	GIMMS dataset	ISLSCP II (Tucker et al., 2005, Hall <i>et al.</i> , 2006)	0.25 degrees	year 2002	Normalized difference vegetation index (NDVI)
Land-use	MODIS dataset	ISLSCP II (Friedl et al.,	0.25 degrees	year 2002	Land use fractions

---

2010, Hall *et al.*, 2006)

---

Table 2. Fractal parameters and the resulting mean global slopes before and after applying the fractal method on the different DEMs; Increase of slope means the increase of the average global slope of a DEM after applying the fractal method; difference after scaling =  $\frac{\theta_{scaled(DEM)} - \theta_{scaled(GTOPO30)}}{\theta_{scaled(GTOPO30)}} * 100$ ; difference before scaling =  $\frac{\theta_{(DEM)} - \theta_{(GTOPO30)}}{\theta_{(GTOPO30)}} * 100$

DEM	resolution arc-minute	standard deviation of elevation m	mean $D$	mean $\alpha_{steepest}$	$\theta$ m m-1	$\theta_{scaled}$ m m-1	Increase of $\theta$ %	difference after scaling %	difference before scaling %
GTOPO30	0.5	570	1.32	0.99	0.023	0.059	61	0	0
ETOPO1	1	530	1.35	1.08	0.016	0.057	71.9	-3.4	-30.4
ETOPO2	2	549	1.37	1.17	0.011	0.055	80	-6.8	-52.2
ETOPO5	5	562	1.42	1.25	0.006	0.054	88.9	-8.5	-73.9

Table 3. Description of Köppen climate symbols and defining criteria (from Peel et al., 2007).

1st	2nd	3rd	Description	Criteria*
<u>A</u>	-	-	<u>Tropical</u>	$T_{cold} \geq 18$
-	<u>f</u>	-	- <u>Rainforest</u>	$P_{dry} \geq 60$
-	-	-		$Not (Af) \ \& \ P_{dry} \geq 100 -$
-	<u>m</u>	-	- <u>Monsoon</u>	$MAP/25$
-	<u>w</u>	-	- <u>Savannah</u>	$Not (Af) \ \& \ P_{dry} < 100 - MAP/25$
<u>B</u>	-	-	<u>Arid</u>	$MAP < 10 \times P_{threshold}$
-	<u>W</u>	-	- <u>Desert</u>	$MAP < 5 \times P_{threshold}$
-	<u>S</u>	-	- <u>Steppe</u>	$MAP \geq 5 \times P_{threshold}$
-	-	<u>h</u>	▪ <u>Hot</u>	$MAT \geq 18$
-	-	<u>k</u>	▪ <u>Cold</u>	$MAT < 18$
<u>C</u>	-	-	<u>Temperate</u>	$T_{hot} > 10 \ \& \ 0 < T_{cold} < 18$
-	<u>s</u>	-	- <u>Dry Summer</u>	$P_{sdry} < 40 \ \& \ P_{sdry} < P_{wwet}/3$
-	<u>w</u>	-	- <u>Dry Winter</u>	$P_{wdry} \leq P_{swet}/10$
-	<u>f</u>	-	- <u>Without dry season</u>	$Not (Cs) \ or \ (Cw)$
-	-	<u>a</u>	▪ <u>Hot Summer</u>	$T_{hot} \geq 22$
-	-	<u>b</u>	▪ <u>Warm Summer</u>	$Not (a) \ \& \ T_{mon10} \geq 4$
-	-	<u>c</u>	▪ <u>Cold Summer</u>	$Not (a \ or \ b) \ \& \ 1 \leq T_{mon10} < 4$
<u>D</u>	-	-	<u>Cold</u>	$T_{hot} > 10 \ \& \ T_{cold} \leq 0$
-	<u>s</u>	-	- <u>Dry Summer</u>	$P_{sdry} < 40 \ \& \ P_{sdry} < P_{wwet}/3$
-	<u>w</u>	-	- <u>Dry Winter</u>	$P_{wdry} < P_{swet}/10$
-	<u>f</u>	-	- <u>Without dry season</u>	$Not (Ds) \ or \ (Dw)$
-	-	<u>a</u>	▪ <u>Hot Summer</u>	$T_{hot} \geq 22$
-	-	<u>a</u>	▪ <u>Warm Summer</u>	$Not (a) \ \& \ T_{mon10} \geq 4$
-	-	<u>c</u>	▪ <u>Cold Summer</u>	$Not (a, \ b \ or \ d)$
-	-	<u>d</u>	▪ <u>Very Cold Winter</u>	$Not (a \ or \ b) \ \& \ T_{cold} \leq -38$
<u>E</u>	-	-	<u>Polar</u>	$T_{hot} < 10$
-	<u>T</u>	-	- <u>Tundra</u>	$T_{hot} > 0$
-	<u>F</u>	-	- <u>Frost</u>	$T_{hot} \leq -0$

Formatted: Font: (Default) Times New Roman, 12 pt

Formatted: Space After: 10 pt

Formatted: Font: (Default) Times New Roman

\* MAP = mean annual precipitation, MAT = mean annual temperature,  $T_{hot}$  = temperature of the hottest month,  $T_{cold}$  = temperature of the coldest month,  $T_{mon10}$  = number of months where the temperature is above 10,  $P_{dry}$  = precipitation of the driest month,  $P_{sdry}$  = precipitation of the driest month in summer,  $P_{wdry}$  = precipitation of the driest month in winter,  $P_{swet}$  = precipitation of the wettest month in summer,  $P_{wwet}$  = precipitation of the wettest month in winter,  $P_{threshold}$  = varies according to the following rules (if 70% of MAP occurs in winter then  $P_{threshold} = 2 \times MAT$ , if 70% of MAP occurs in summer then  $P_{threshold} = 2 \times MAT + 28$ , otherwise  $P_{threshold} = 2 \times MAT + 14$ ). Summer (winter) is defined as the warmer (cooler) six month period of ONDJFM and AMJJAS.

Formatted: Font: (Default) Times New Roman

Formatted: Suppress line numbers



Table 34. Linear multiple regression equations for different climate zones, relating high resolution erosivity from the USA with one or more significant parameters: annual total mean precipitation ( $P$ ), mean elevation ( $z$ ) and the simple precipitation intensity index ( $SDII$ )

Climate zone	Explaining parameters	Regression function - optimal	$R^2$	Residual standard error
BWk	P, SDII	$R = 0.809 * P^{0.957} + 0.000189 * SDII^{6.285}$		
BSh	P, SDII	$\log R = -7.72 + 1.595 * \log P + 2.068 * \log SDII$	0.97	0.22
Bsk	P, SDII, Z	$\log R = 0.0793 + 0.887 * \log P + 1.892 * \log SDII - 0.429 * \log Z$	0.89	0.35
Csb	P	$R = 98.35 + 0.000355 * P^{1.987}$		0.16
Cfa	P, SDII, Z	$\log R = 0.524 + 0.462 * \log P + 1.97 * \log SDII - 0.106 * \log Z$	0.89	0.11
Cfb	P, SDII	$\log R = 4.853 + 0.676 * \log P + 3.34 * \log SDII$	0.97	0.21
Dsa	Z, SDII	$\log R = 8.602 - 0.963 * \log SDII - 0.247 * \log Z$	0.51	0.05
Dsb	P	$\log R = 2.166 + 0.494 * \log P$	0.45	0.25
Dsc	SDII	$\log R = 6.236 - 0.869 * \log SDII$	0.51	0.02
Dwa	P	$\log R = -0.572 + 1.238 * \log P$	0.99	0.02
Dwb	P, SDII	$\log R = -1.7 + 0.788 * \log P + 1.824 * \log SDII$	0.98	0.02
Dfa	P, SDII	$\log R = -1.99 + 0.737 * \log P + 2.033 * \log SDII$	0.9	0.16
Dfb	P, SDII, Z	$\log R = -0.5 + 0.266 * \log P + 3.1 * \log SDII - 0.131 * \log Z$	0.89	0.32
Dfc	SDII	$\log R = -1.259 + 3.862 * \log SDII$	0.91	0.23
ET	P	$\log R = -3.945 + 1.54 * \log P$	0.14	0.42
EF+EFH	P	$\log R = 16.39 - 1.286 * \log P$	0.6	0.13

---

ETH	P, SDII	$\log R = 21.44 + 1.293 * \log P - 10.579 * \log SDII$	0.52	0.53
-----	---------	--	------	------

---

Table 45. Linear multiple regression equations for different climate zones for regions that have no data on the simple precipitation intensity index (*SDII*). The regression equations relate high resolution erosivity from the USA with the annual total mean precipitation (*P*) and/or the mean elevation (*z*)

Climate zone	Optimal regression function (when <i>SDII</i> is not available)	R <sup>2</sup>	Residual standard error
BWk	Method Renard & Freimund (1994)		
BSh	$\log R = -8.164 + 2.455 * \log P$	0.86	0.5
BSk	$\log R = 5.52 + 1.33 * \log P - 0.977 * \log Z$	0.76	0.52
Cfa	$\log R = 3.378 + 0.852 * \log P - 0.191 * \log Z$	0.57	0.23
Cfb	$\log R = 5.267 + 0.839 * \log P - 0.635 * \log Z$	0.81	0.5
Dsa	$\log R = 7.49 - 0.0512 * \log P - 0.272 * \log Z$	0.48	0.06
Dsc	$\log R = 4.416 - 0.0594 * \log P$	0.015	0.03
Dwb	$\log R = 1.882 + 0.819 * \log P$	0.81	0.08
Dfa	$\log R = -2.396 + 1.5 * \log P$	0.65	0.29
Dfb	$\log R = 1.96 + 1.084 * \log P - 0.34 * \log Z$	0.74	0.48
Dfc	$\log R = -3.263 + 1.576 * \log P$	0.56	0.49
ETH	$\log R = -10.66 + 2.43 * \log P$	0.4	0.59

Table 56. Mean high resolution *R* values from the USA and Switzerland and mean modelled *R* values with uncertainty range for each addressed climate zone

**Comment [VN12]:**  
**Comment [5]: Reviewer #1:**  
 Can you show R results by the unadjusted model for comparison?  
**Reply:** Yes, see the new table

<u>climate</u>	<u>description</u>	<u>observed</u> <i>R</i> mean	<u>old</u> <u>method</u> <i>R</i> mean	<u>adjusted</u> <u>method</u> <i>R</i> mean	<u>Adjusted method</u> <u>uncertainty range</u>
BWk	arid, desert, cold	284	533	291	158-495
BSh	arid, steppe, hot	2168	1356	2207	1723-2828
BSk	arid, steppe, cold	876	884	885	749-1046
Csb	temperate, dry warm summer	192	1136	192	133-292
Cfa	temperate, without dry season, hot summer	5550	5607	5437	4830-6123
Cfb	temperate, without dry season, warm summer	1984	5359	1971	1431-2715
Dsa	cold, dry hot summer	172	445	171	86-340
Dsb	cold, dry warm summer	175	896	168	151-187
Dsc	cold, dry cold summer	115	374	115	91-145
Dwa	cold, dry winter, hot summer	1549	1444	1551	1280-1879
Dwb	cold, dry winter, warm summer	1220	1418	1214	1057-1395
Dfa	cold, without dry season, hot summer	2572	2983	2582	2346-2843
Dfb	cold, without dry season, warm summer	1101	1798	1124	922-1371
Dfc	cold, without dry season, cold summer	483	701	483	423-552
ET	polar, tundra	1352	6257	1249	23-68088
EF+EFH	polar, frost + polar, frost, high elevation	1468	5469	1450	16-132001
ETH	polar, tundra, high elevation	945	5580	832	0-6314918

Formatted Table

<u>climate</u>	<u>description</u>	<u>observed</u> <i>R</i> mean	<u>modelled</u> <i>R</i> mean	<u>modelled</u> <u>uncertainty range</u>
BWk	arid, desert, cold	284	291	158-495
BSh	arid, steppe, hot	2168	2207	1723-2828
BSk	arid, steppe, cold	876	885	749-1046
Csb	temperate, dry warm summer	192	192	133-292
Cfa	temperate, without dry season, hot summer	5550	5437	4830-6123
Cfb	temperate, without dry season, warm summer	1984	1971	1431-2715

Formatted Table

Dsa	cold, dry hot summer	172	171	86-340
Dsb	cold, dry warm summer	175	168	151-187
Dsc	cold, dry cold summer	115	115	91-145
Dwa	cold, dry winter, hot summer	1549	1551	1280-1879
Dwb	cold, dry winter, warm summer	1220	1214	1057-1395
Dfa	cold, without dry season, hot summer	2572	2582	2346-2843
Dfb	cold, without dry season, warm summer	1101	1124	922-1371
Dfc	cold, without dry season, cold summer	483	483	423-552
ET	polar, tundra	1352	1249	23-68088
EF+EFH	polar, frost + polar, frost, high elevation	1468	1450	16-132001
ETH	polar, tundra, high elevation	945	832	0-6314918

Table 67. Statistics of the comparison of high resolution erosivity from three regions to estimated erosivity from the Renard and Freimund method and the new regression equations

	Observed			Estimated – Renard & Freimund					Estimated – multiple linear regression				
	Range	Mean	Standard deviation	Range	Mean	Standard deviation	Correlation coefficient	Rank correlation coefficient	Range	Mean	Standard deviation	Correlation coefficient	Rank correlation coefficient
Switzerland	121-6500	1204	833	2335-10131	5798	1654	0.51	0.42	225-2572	1256	472	0.49	0.3
the USA (aggregated huc4)	105-4963	1271	1174	57-15183	1870	2088	0.51	0.68	60-15808	1691	2188	0.58	0.83
Ebro basin	40 - 4500	891	622	747 - 5910	1529	846	-	-	167 - 4993	836	701	-	-

Table 78. Comparison of the global erosion rates ( $\text{t ha}^{-1} \text{y}^{-1}$ ) and percentiles between different versions of the RUSLE model

	mean	25th percentile	50th percentile	75th percentile	90th percentile
RUSLE unadjusted	5.1	0.2	0.8	2.8	8.6
RUSLE adjusted with S	11.1	0.3	1.2	4.3	15.7
RUSLE adjusted with R	3.6	0.1	0.6	1.9	6.3
RUSLE adjusted with S & R	7.3	0.2	0.8	3	10.9

Table 89. Statistics of the observed and modelled erosion rates from the unadjusted and adjusted versions of the RUSLE for the USA and Europe ( $t\ ha^{-1}\ y^{-1}$ )

Region	Source	Observations			Adjusted RUSLE			Unadjusted RUSLE		
		Range	Mean	Standard deviation	Range	Mean	Standard deviation	Range	Mean	Standard deviation
Europe (Aggregation country level) no small countries	Cerdan et al., 2010	0.1-2.6	0.9	0.7	0.1-7	2.3	2.1	0-14	2.8	3.6
the USA (Aggregation HUC4 level)	NRI database	0-11	1.7	2.1	0.2-21	1.7	2.5	0-14	1.9	2.3



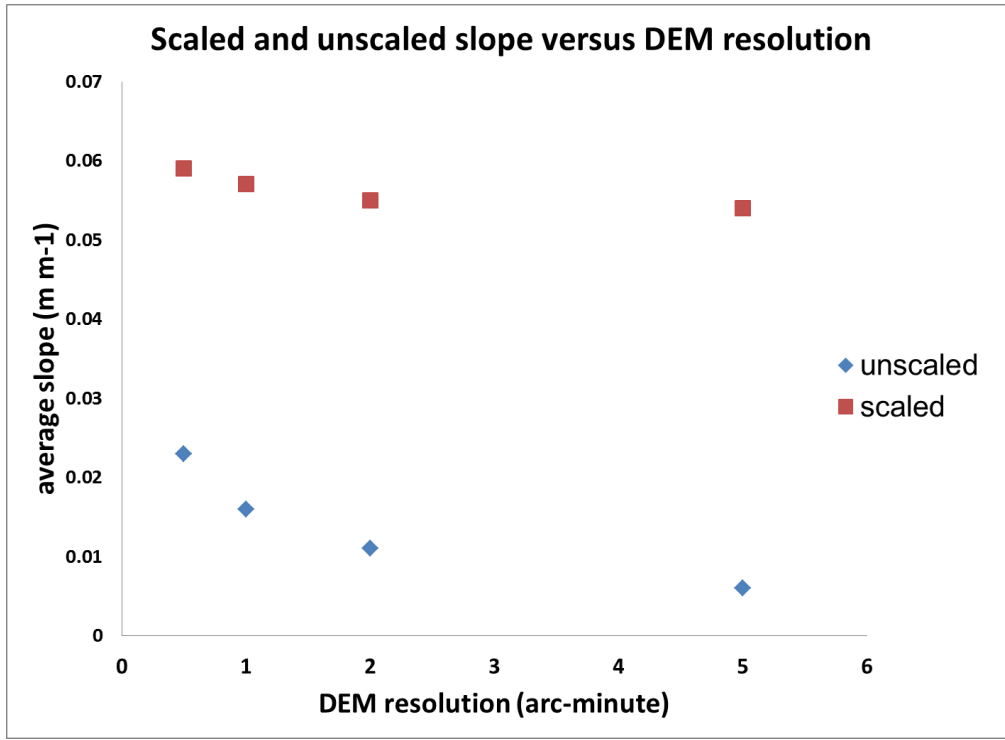
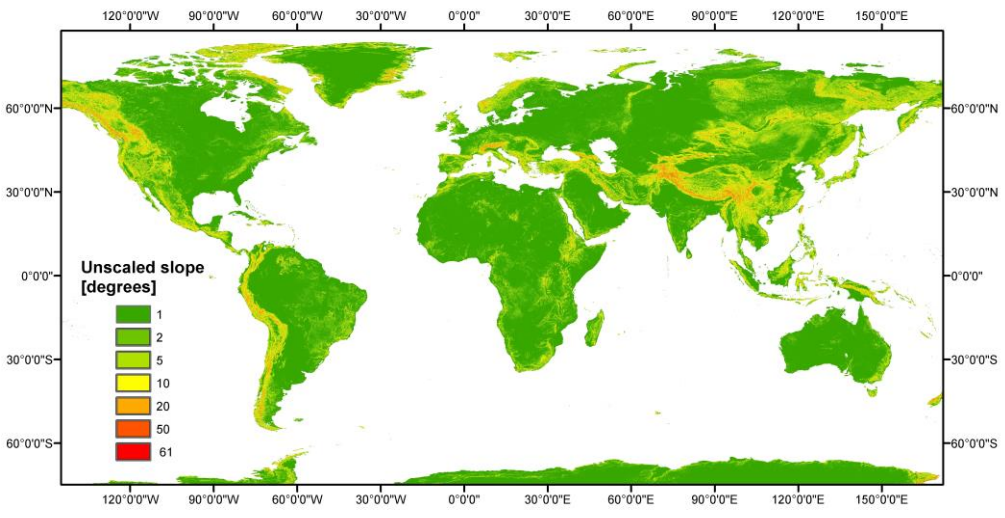


Figure 1. Global average unscaled slope estimated from different coarse resolution digital elevation models (DEMs) as function of their resolution (blue); and global average scaled slope from the same DEMs as function of their resolution (red).

(A)



(B)

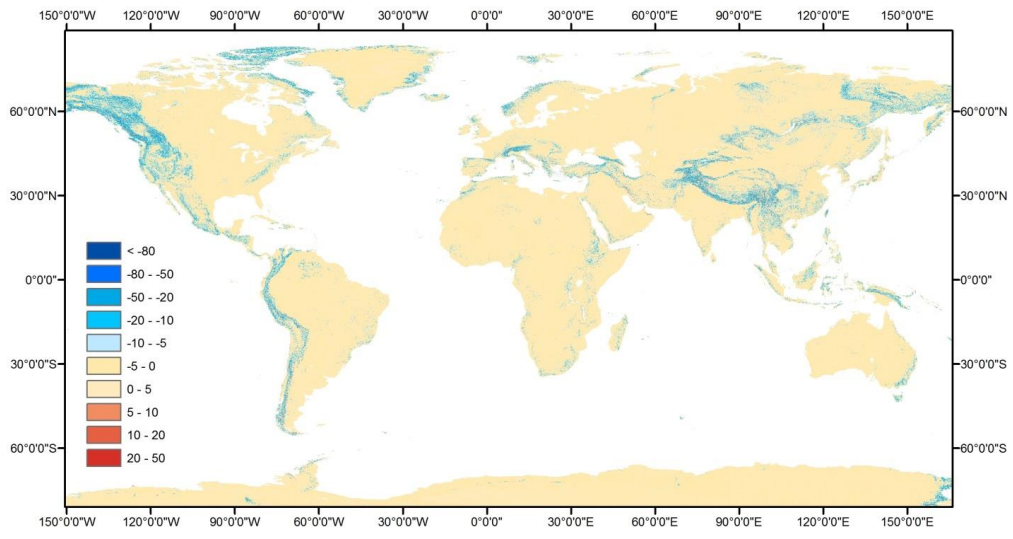


Figure 2. (A) A global map of the unscaled slope derived from the 30 arc-second DEM using a target resolution of 150m; (B) A global map showing the difference between the unscaled and scaled slopes (in degrees), where blue colours show an underestimation by the unscaled slope when compared to the scaled slope and reddish colours show an overestimation.

**Comment [VN13]:**

**Comment [5]: Reviewer #2:** I would find it useful if the original RUSLE estimation was shown as well as a difference. Figure 2: caption 'redisch'

**Reply:** We add in the revised manuscript the unscaled global slope in Figure 2A and keep the difference plot in Figure 2B. "Redisch" is corrected by "Reddish" now.

**Formatted:** Font: (Default) Times New Roman

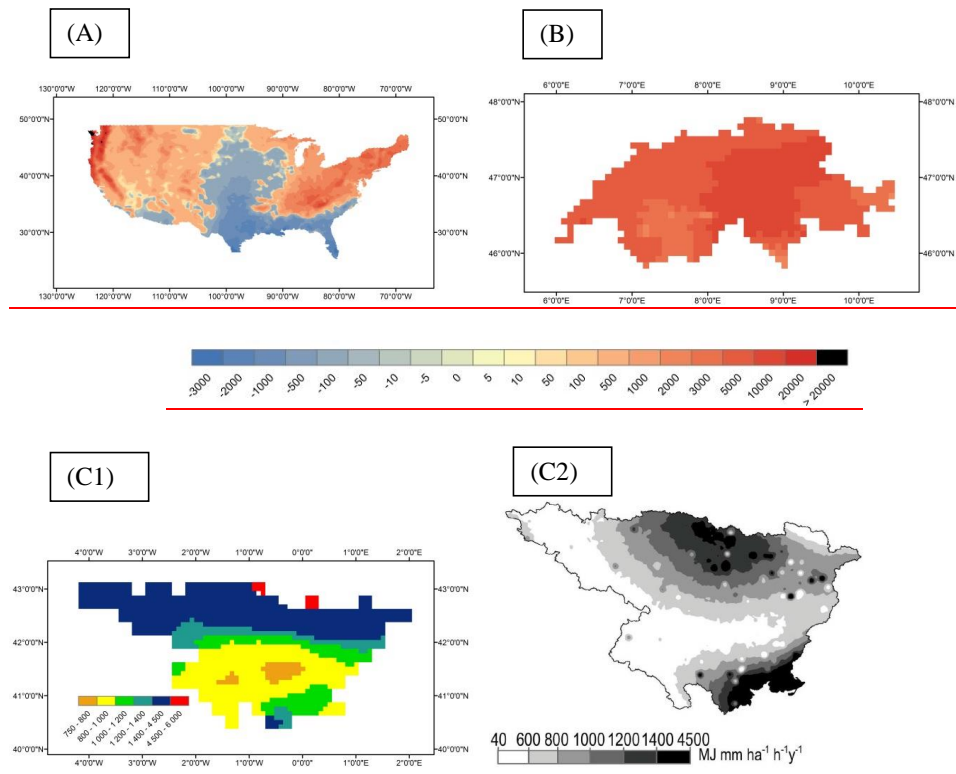


Figure 3. Spatial difference plots showing the difference between the high resolution erosivity and erosivity calculated with the method of Renard and Freimund for (A) the USA, (B) Switzerland and (C) the Ebro basin in Spain; In (A) and (B) the blue colours show an underestimation of the calculated erosivity when compared to the high resolution erosivity, while the red colours show an overestimation; the Ebro basin serves here as an independent validation

set and it has two graphs, (C1) a spatial plot of erosivity according to Renard and Freimund, and (C2) the high resolution erosivity from Angulo-Martinez et al. (2009); All values in the graphs are in  $\text{MJ mm ha}^{-1} \text{ h}^{-1} \text{ y}^{-1}$

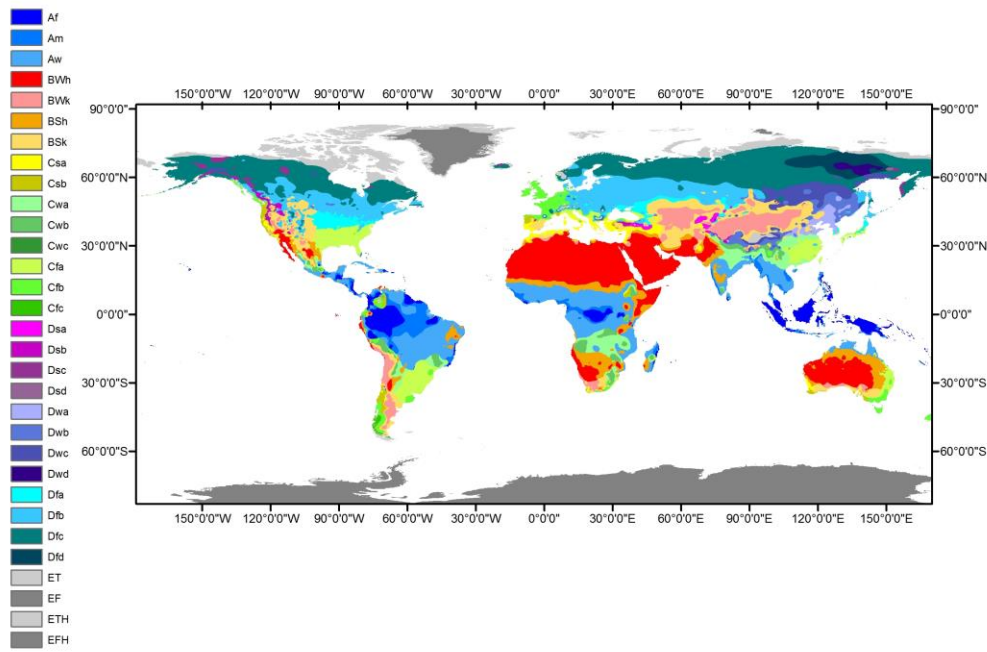
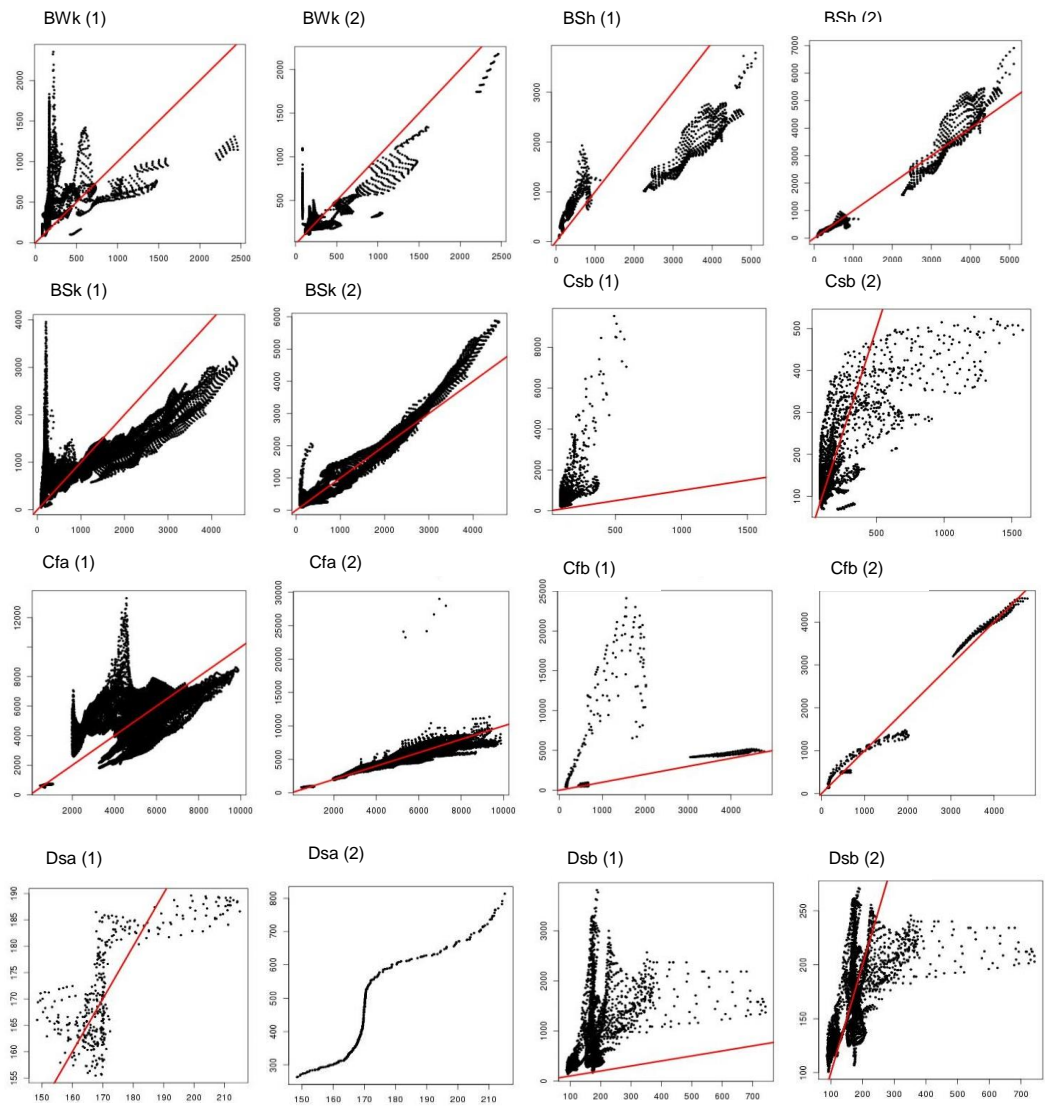


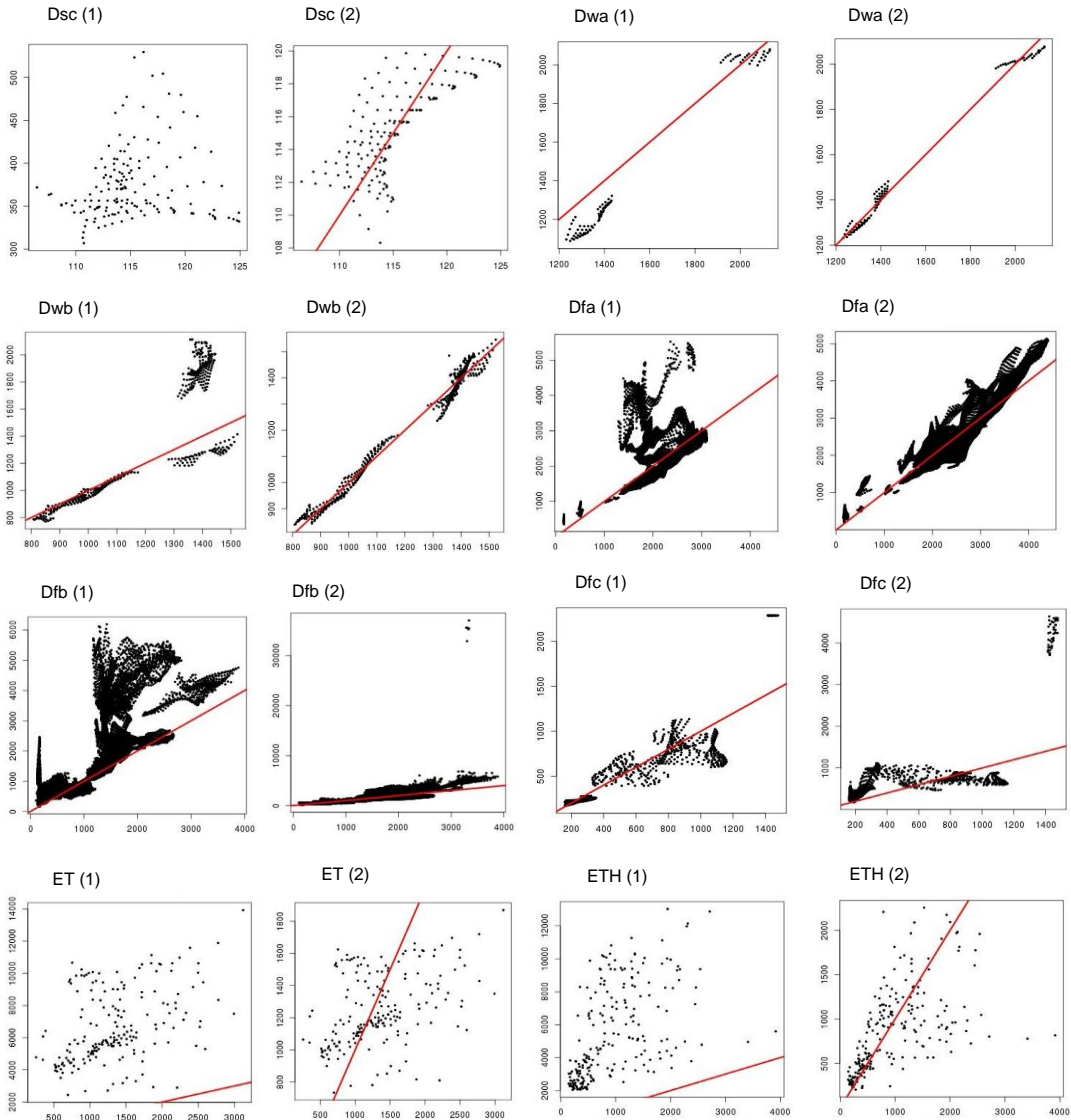
Figure 4. The Köppen-Geiger climate classification global map with resolution of 5 arc-minute (Peel et al., 2007)

**Comment [VN14]:**

**Comment [7]: Reviewer #2:** more explanation of figure in the caption would be useful.

**Reply:** We add an additional table (Table 3) with definitions for all climate zones as presented in Peel et al. (2007) in the revised manuscript. The rest of the tables in the manuscript are renumbered.





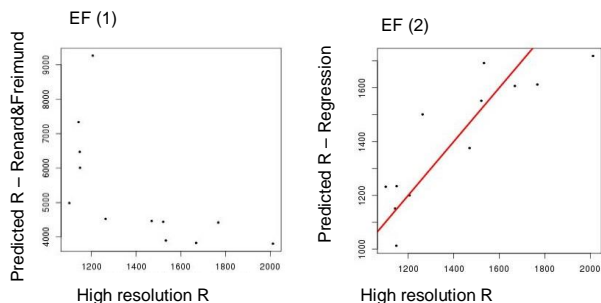


Figure 5. Comparison of high resolution erosivity data and predicted erosivity from (1) the Renard and Freimund method and (2) the new regression equations, for various climate zones; the red line is the 1 to 1 line that always lies on the 45 degree diagonal, and does not appear in some graphs because predicted erosivity is overestimated; All values in the graphs are in MJ mm ha<sup>-1</sup> h<sup>-1</sup> y<sup>-1</sup>

**Comment [VN15]:**

**Comment [11]: Reviewer #2:** Figures 5 needs to be improved. The layout and sizing of the plots needs to be consistent. I would find it easier to evaluate the results if the plots were given equal axes such that the one-to-one line always lies on the 45 degree diagonal, and the axes were the same between 1 and 2. Units should be mentioned

**Reply:** The sizing of figures 5 is improved to be more consistent in the revised manuscript. It was for us difficult to give all the plots equal axes, due to the fact that the correlation becomes much less visible. Also one is not able to see anymore how the data is spread, and in which way the different methods overestimate or underestimate the observed R values. In these plots it is most important to see how the observed R values correlate with the modelled ones from the different methods for a specific climate zone. In some cases the modelled R values are much larger than the observed ones, which make it difficult to use equal axes and equal spacing between the axis ticks. Finally, one needs to keep in mind that the red line always lays on the 45 degree diagonal. In the description of figure 5 in the revised manuscript we add the units and explicitly mention that the red line always lies on the 45 degree diagonal.

**Formatted:** Font: Times New Roman, 12 pt

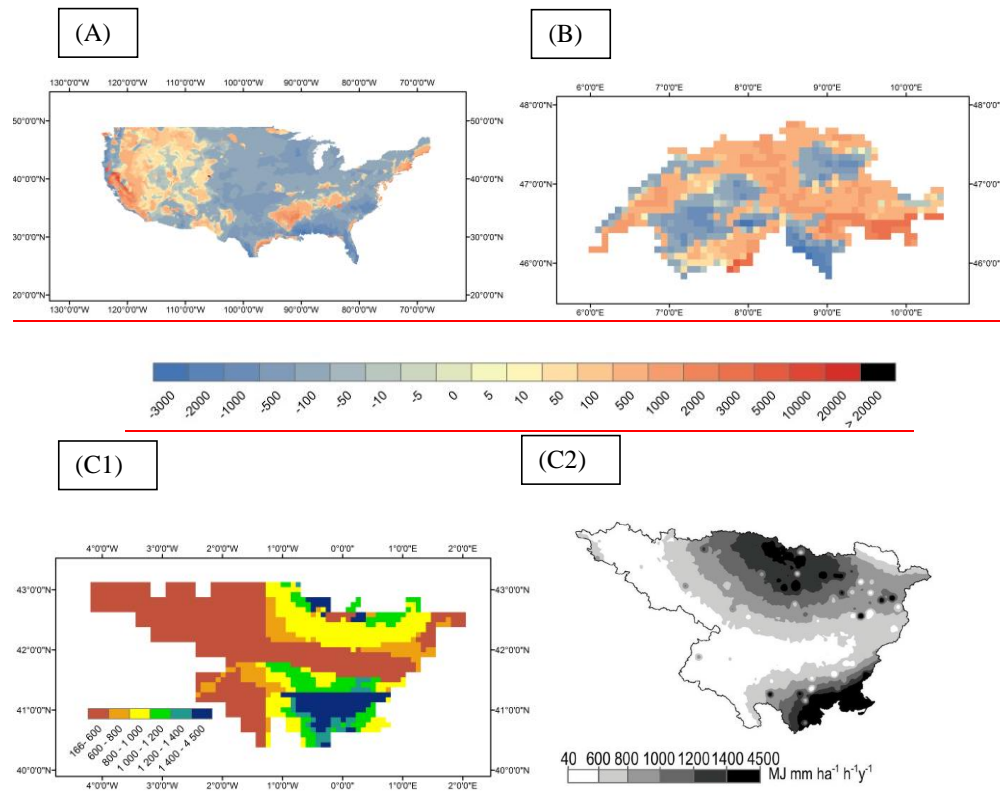


Figure 6. Spatial difference plots showing the difference between the high resolution rainfall

erosivity and erosivity calculated with the new regression equations for (A) the USA, (B) Switzerland and (C) the Ebro basin in Spain; In (A) and (B) the blue colours show an underestimation of the calculated erosivity when compared to the high resolution erosivity, while the red colours show an overestimation; the Ebro basin serves here as an independent validation set and it has two graphs, (C1) a spatial plot of erosivity according to the new regression equations, and (C2) the high resolution erosivity from Angulo-Martinez et al. (2009); All values in the graphs are in  $\text{MJ mm ha}^{-1} \text{h}^{-1} \text{y}^{-1}$ ; The Ebro basin is presented differently here when compared to the USA and Switzerland, due to the lack of the original erosivity data from Angulo-Martinez et al., 2009.

**Comment [VN16]:**

**Comment [6]: Reviewer #2:** Why is Switzerland presented differently to the other two regions? I would prefer a uniform representation, unless there is a rational for this, in which case it should be presented.

**Reply:** We guess you mean not Switzerland but the Ebro basin in Spain that is presented differently. This is due to the fact that we cannot have access to the original erosivity data of the Ebro basin (presented in the study of Angulo-Martinez et al., 2009) and thus cannot make a difference plot such as the figures of the USA and Switzerland. We state this now in the description of figure 6.



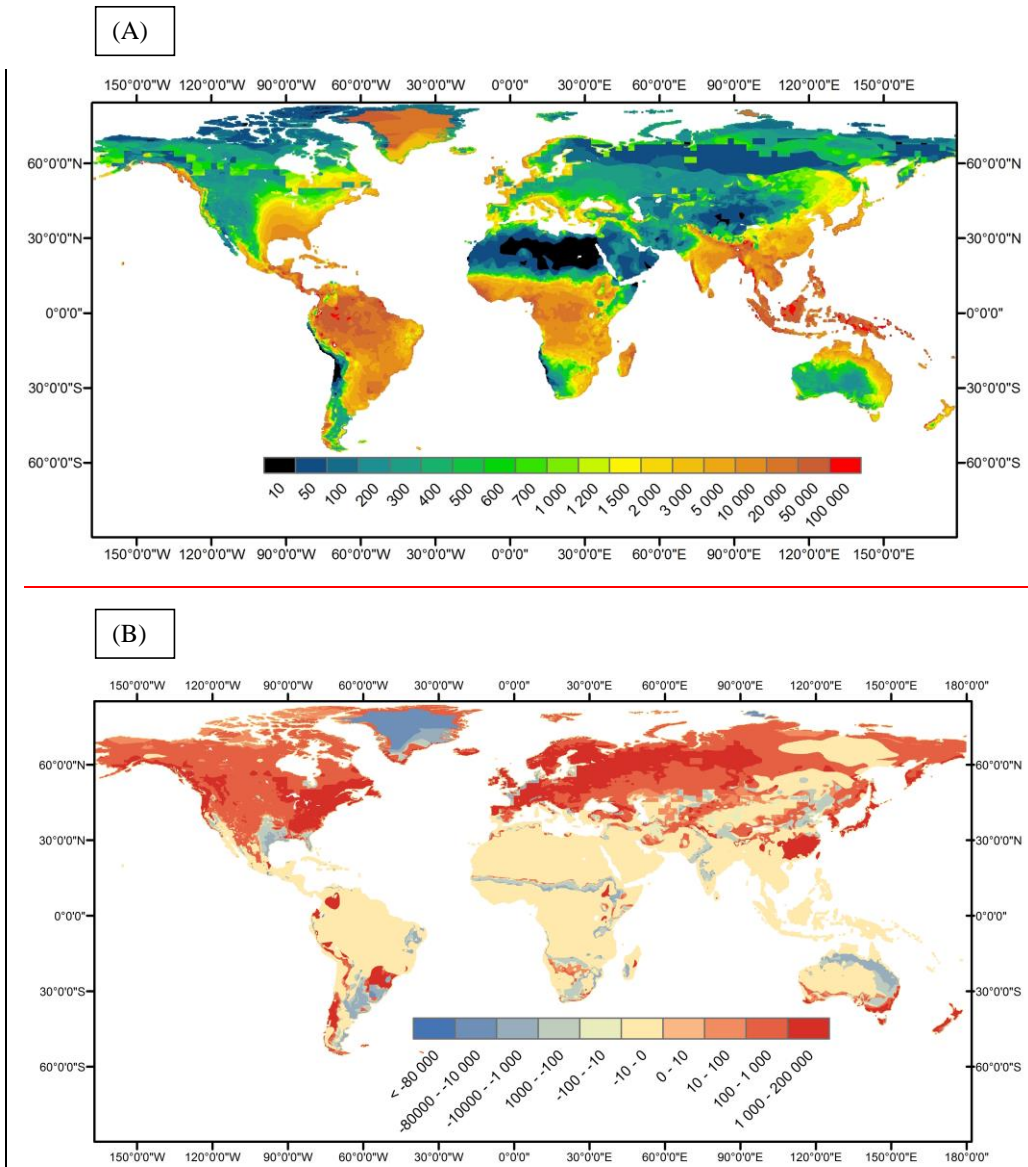
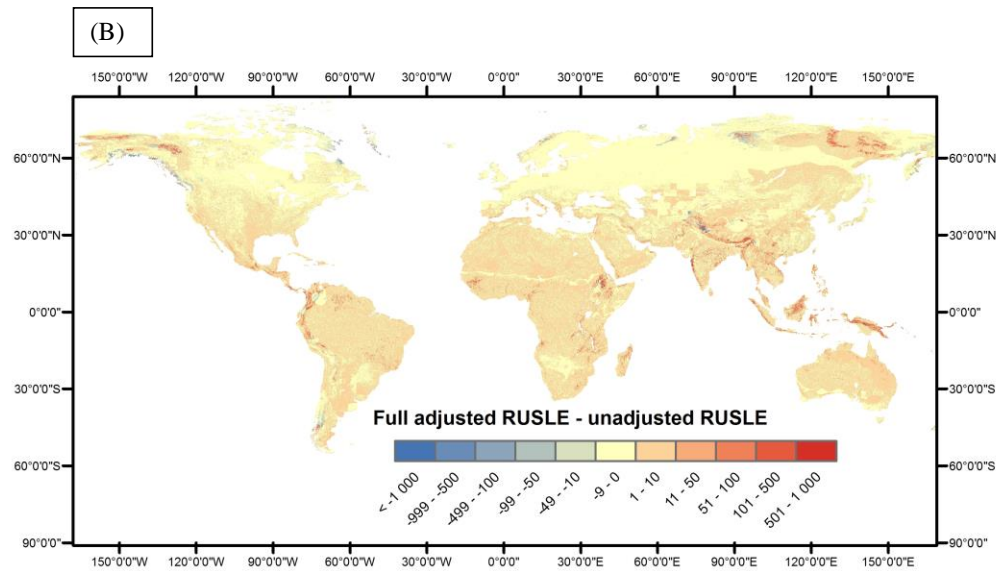
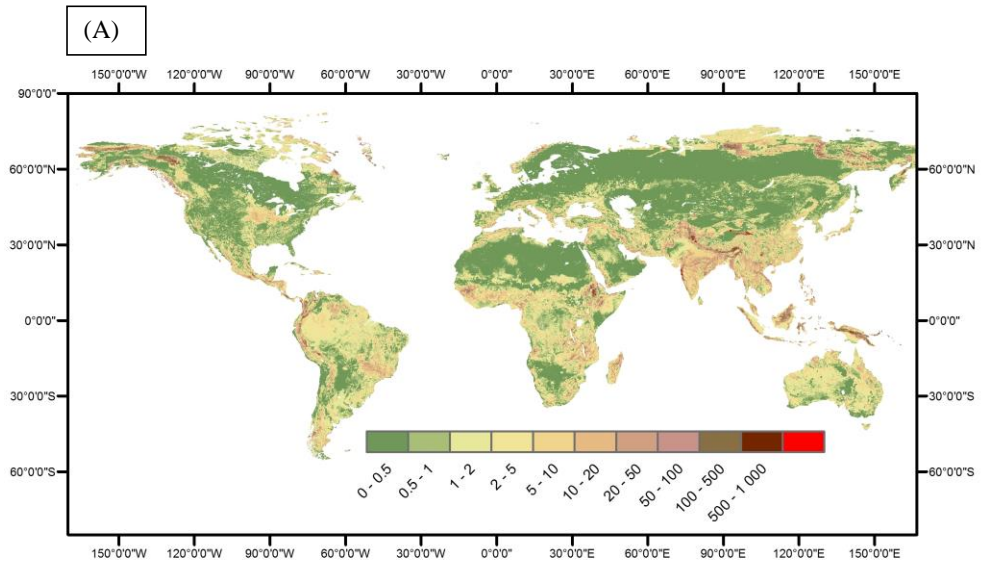


Figure 7. (A) Global distribution of the new modelled rainfall erosivity values according to the new regression equations; and (B) a difference map between erosivity calculated according to the method of Renard and Freimund and the new modelled erosivity values ( $\text{MJ mm ha}^{-1} \text{h}^{-1} \text{y}^{-1}$ ),

where blue colours indicate lower erosivity values by Renard and Freimund, while redish colours indicate higher erosivity values; map resolution is 5 arc-minute



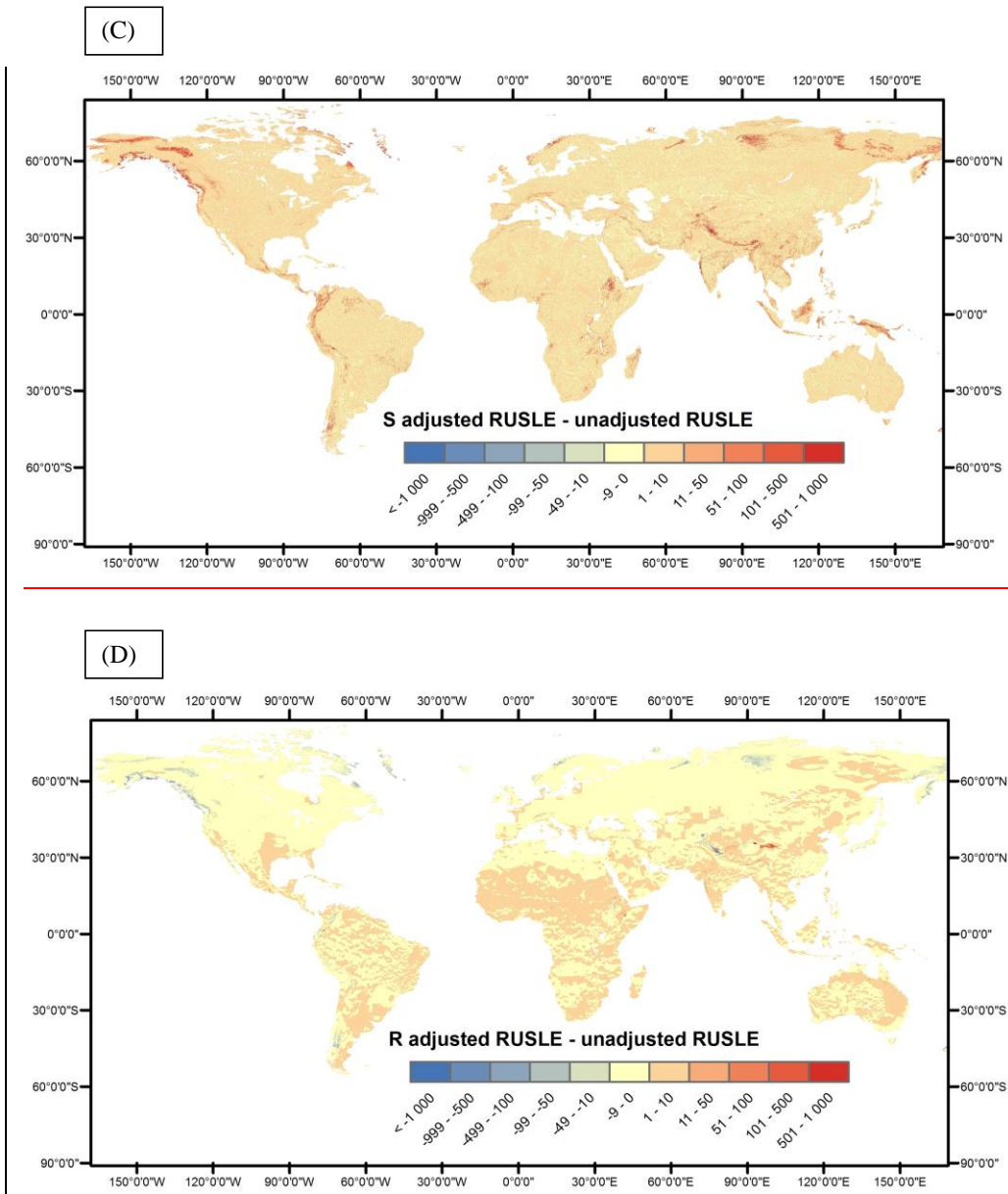
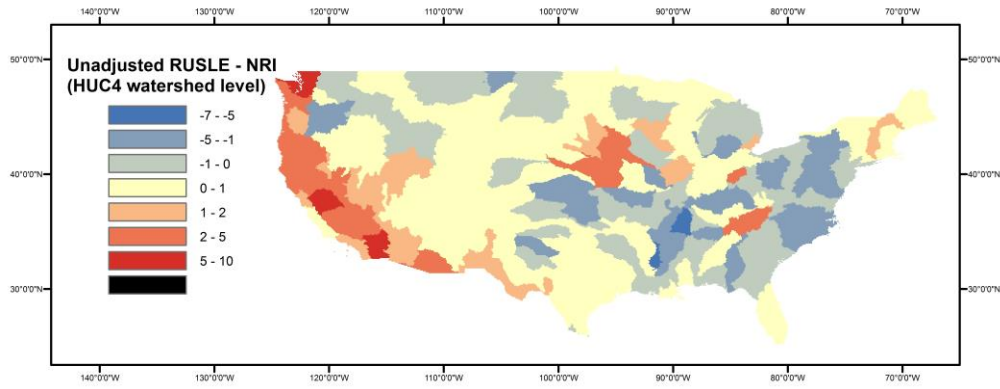


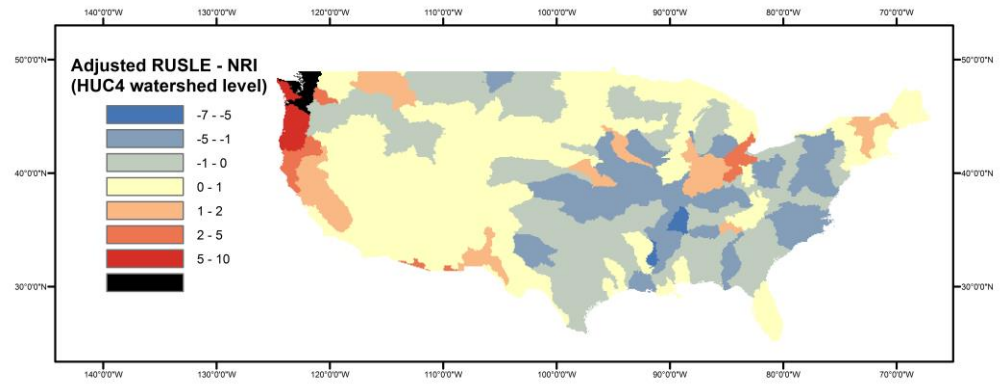
Figure 8. (A) Global yearly averaged erosion rates according to the fully adjusted RUSLE model; (B) a difference map between the fully adjusted and unadjusted RUSLE model; (C) a difference map between the adjusted S RUSLE and the unadjusted RUSLE model; (D) a difference map between the adjusted R RUSLE and the unadjusted RUSLE model; in figures

B,C and D the reddish colors show an overestimation of by the adjusted RUSLE model and yellow to bluish colors show an underestimation; resolution of all maps is 5 arc-minute and the units are in  $t\ ha^{-1}\ y^{-1}$

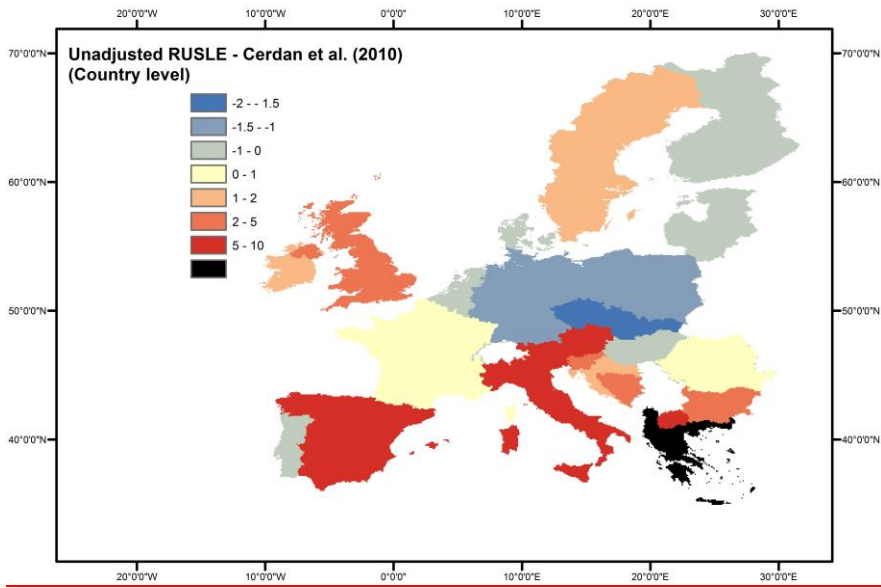
(A1)



(A2)



(B1)



(B2)

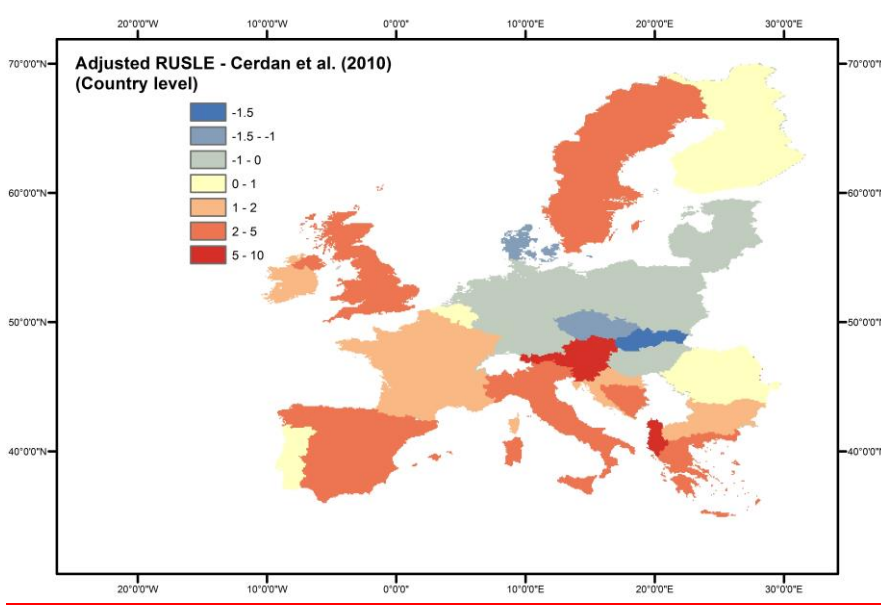


Figure 89. (A) Difference plots between soil erosion estimates from the NRI database for the USA and estimates of (A1) the unadjusted RUSLE model, and of (A2) the adjusted RUSLE model; all aggregated at HUC4 watershed level; (B) Difference plots between soil erosion estimates from the database of Cerdan et al. (2010) for Europe and estimates of (B1) the unadjusted RUSLE model and of (B2) the adjusted RUSLE model; all aggregated at country level; reddish colors represent an overestimation (%) while the bluish represent and underestimation (%) compared to the erosion values from the databases; black color is an overestimation > 10%.